ETH zürich

MaP Graduate Symposium

featuring the MaP Award ceremony

June 5, 2014

HG E5 and E-floor main hall

Rämistrasse 101, ETH Zürich

MaP Competence Center for Materials and Processes

The Competence Center for Materials and Processes would like to thank the following companies for their sponsoring

METTLER TOLEDO

oerlikon balzers

PHONAK life is on

SENSIRION THE SENSOR COMPANY

BIOTRONIK excellence for life

TABLE OF CONTENTS

ETH ZENTRUM: SITE MAP

oral presentations in HG E 5
poster presentations & exhibition in HG main hall

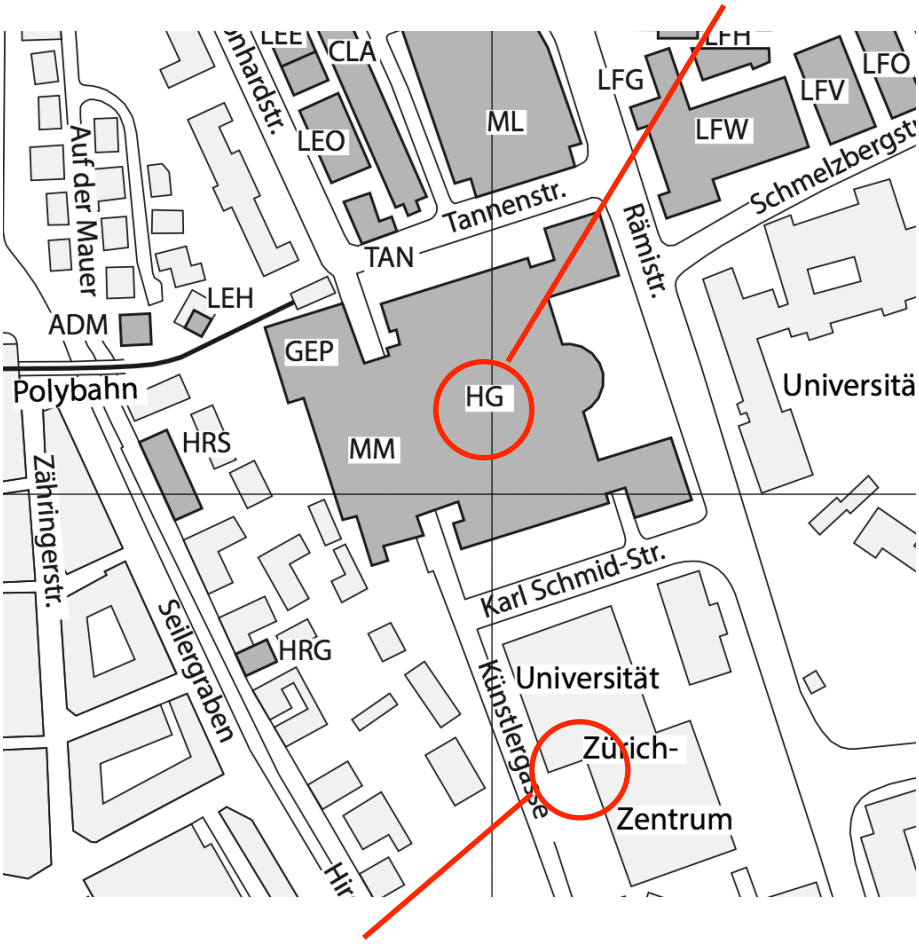

dinner location – Mensa B, Universität Zürich-Zentrum

WLAN access for external guests:

Network: public
Login: MaPGradSymp
Password: MaP2014

HG E-floor

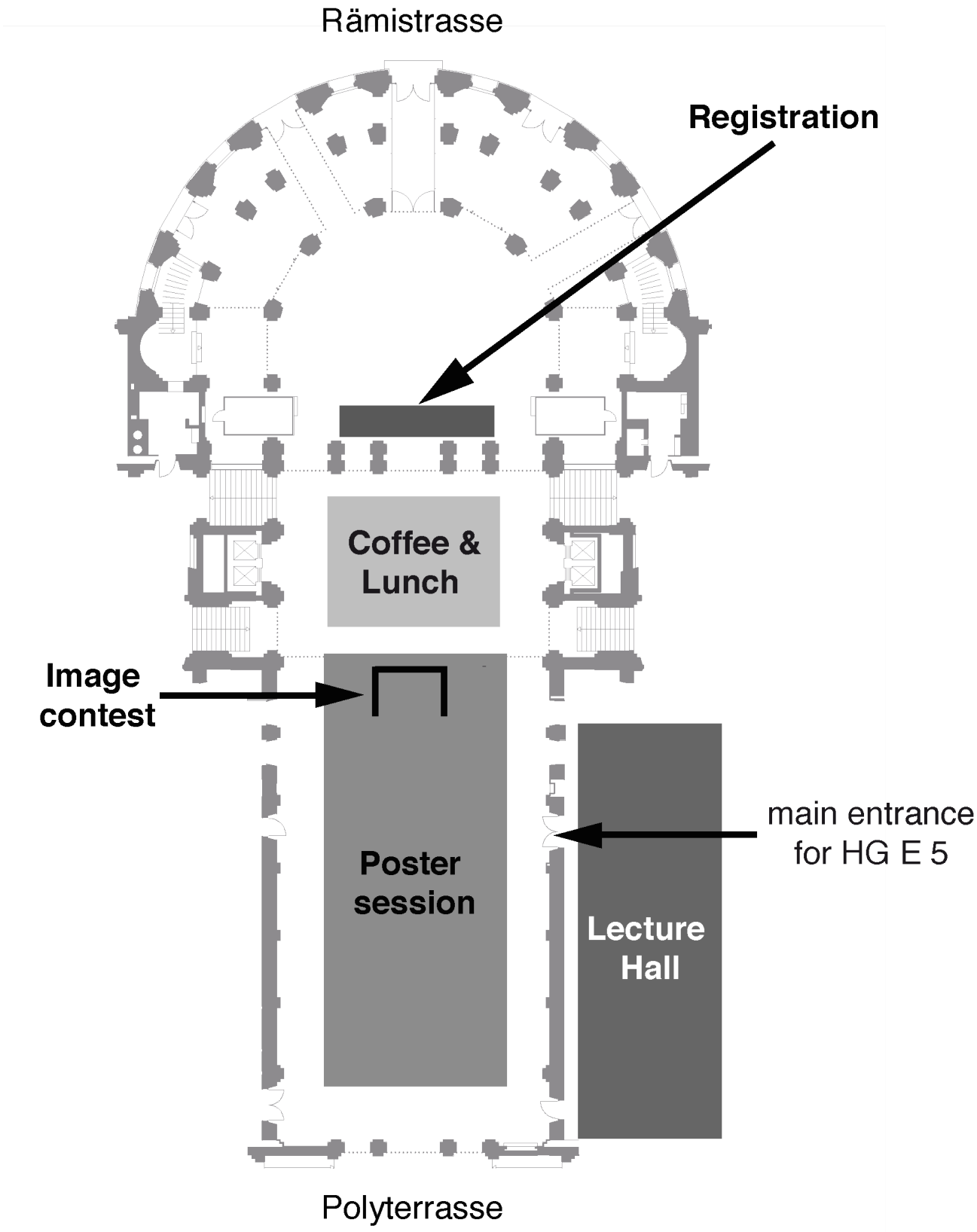
Rämistrasse
Registration
Coffee &
Lunch
Image
contest
Poster
session
Lecture
Hall
main entrance
for HG E 5
Polyterrasse

PROGRAM

08:00	Registration *(entrance hall Rämistrasse)*
08:50	**Prof. André Studart,** *MaP Director* Opening remarks
09:00	**Giulia Tagliabue,** *Thermodynamics in Emerging Technologies, D-MAVT* White Light Harvesting with a Broadband Plasmonic Absorber
09:20	**Franziska Schlich,** *Nanometallurgy, D-MATL* Bright Color Appearance in Ultrathin Semiconductor Layers on a Variety of Substrate Materials
09:40	**Weyde Lin,** *Nanoelectronics, D-ITET* Size-Dependent Properties of Lead Sulfide Nanocrystal Solar-Cells
10:00	**Ivo Leibacher & Peter Reichert,** *Center of Mechanics, D-MAVT* Sound Waves for the Handling of Droplets
10:20	*Coffee Break*
10:30	*Poster Session Part A*
11:00	**Max Kory,** *Polymer Chemistry, D-MATL* Gram-Scale Synthesis of Organic Two-Dimensional Polymer Crystals and Exfoliation into Nanometer-Thin Sheets
11:20	**Ye Tao,** *Spin Physics and Imaging, D-PHYS* Facile Fabrication of Single-Crystal-Diamond Nanostructures with Ultrahigh Aspect Ratio
11:40	**Wolfram Grüning,** *Surface and Interfacial Chemistry, D-CHAB* C–H Activation with Iridium(I) on Bipyridine-Containing Periodic Mesoporous Organosilicas
12:00	**Tommaso Delpero,** *Composite Materials & Adaptive Structures, D-MAVT* Adaptive Materials for Programmable Metamaterials
12:20	*Lunch & Poster Session* *13:00 – 13:30 Part B* *13:30 – 14:00 Part C*

MaP Award 2014	
14:00	**Dr. Johannes Haberl,** *Food and Soft Materials, D-HEST* Magnetic Liquid Crystalline Elastomers
14:20	**Dr. Martina Hitzbleck,** *Biosensors and Bioelectronics, D-ITET* Advanced Capillary-Driven Microfluidic Chips for Diagnostic Applications
14:40	**Dr. Rafael Libanori,** *Complex Materials, D-MATL* Bioinspired Composites with Controlled Alignment and Distribution of Anisotropic Reinforcing Particles
15:00	**Dr. Matthias Muoth,** *Micro and Nanosystems, D-MAVT* Clean Integration of Single-Walled Carbon Nanotubes for Electromechanical Systems
15:20	*Coffee Break*
15:50	**Nicolas Broguiere,** *Cartilage Engineering and Regeneration, D-HEST* Synthetic Extracellular Matrix for 3D Cultures of Central Neurons
16:10	**Dr. Kiran Chikkadi,** *Micro and Nanosystems, D-MAVT* Ultra-Low Power Gas Sensors Using Carbon Nanotubes
16:30	**Dr. Niko Münzenrieder,** *Wearable Computing, D-ITET* Electronic Membrane
16:50	Flash Poster Presentations
17:05	Industries Presentations
17:45	Award ceremonies: Image Contest, Poster Prize, MaP Award
18:00	*Industry Apéro*
19:15	*Dinner at Uni Mensa*

ABSTRACTS OF ORAL PRESENTATIONS

Session 1: 09:00 – 10:20

Giulia Tagliabue, H. Eghlidi and D. Poulikakos

Thermodynamics in Emerging Technologies, D-MAVT

White Light Harvesting with a Broadband Plasmonic Absorber

Metallic nanostructures supporting localized or propagating surface plasmons are the founding elements of nano-photonic devices due to their ability to concentrate and manipulate light at nanoscale dimensions, well below the diffraction limit. Indeed, upon excitation of a surface plasmon resonance, the optical size of a metallic nanostructure becomes much larger than its nanoscopic physical size allowing an efficient coupling with light. At the same time, due to the evanescent nature of the plasmon waves, fields are squeezed into nano-volumes in the proximity of the structure and consequently get largely enhanced.
Several energy-related applications such as solar cells, thermo-photovoltaic, thermoelectric and photocatalysis, would greatly benefit from these light-harvesting and concentration properties as well as of the sub wavelength dimensions of the resulting structure. However, due to their resonant behavior, plasmonic nanostructures normally exhibits a limited spectral bandwidth where efficient light-matter interaction occurs and are thus not suitable for white light harvesting. Furthermore, most applications require large area structures which are difficult to achieve with standard nanoscale fabrication techniques.
Here, we present an ultrathin (260 nm), broadband plasmonic absorber with average absorption of 88% within the spectral range 380 - 980 nm. It consists of a metal (Au) - insulator (SiO_2) – metal (Au) (MIM) structure with a front pattern consisting of a hexagonal array of tapered triangles. The wide absorption bandwidth was obtained exploiting four distinct plasmonic absorption phenomena, two of which related to the MIM configuration and the other two supported by the front triangular structure. We show how, after investigating their dependence on the geometrical parameters of the structure, we were able to combine the collective benefit of these resonances and piece together a continuous absorption band. Furthermore, the chosen fabrication process is compatible with large scale, roll-to-roll procedures, making our design a valuable candidate for white light harvesting applications.

Franziska Schlich and R. Spolenak

Nanometallurgy, D-MATL

Bright Color Appearance in Ultrathin Semiconductor Layers on a Variety of Substrate Materials

Ultrathin semiconductor layers on metals are attractive systems because they result in bright color appearances. These colors are caused by absorption resonances in 5 nm to 30 nm thick semiconductor layers. The thickness is considerably reduced compared to conventional transparent dielectric optical coatings whose thicknesses are on the order of the wavelength of the light.
We demonstrate that the underlying material is not only limited to metals as assumed previously. Instead, it can be replaced by any material by using multiple layers that effectively mimic the optical constant of a highly reflective metal. We show that the resulting color is strongly dependent on the refractive indices of the materials. Therefore, the coatings show a large color contrast between the amorphous and the crystalline phase of the semiconductor. Hence, these coatings could be promising candidates for data storage.

Weyde Lin*, D. Bozyigit*, O. Yarema, S. Volk and V. Wood

Nanoelectronics, D-ITET

Size-Dependent Properties of Lead Sulfide Nanocrystal Solar-Cells

One of the key motivations in using colloidally synthesized nanocrystals for optoelectronic devices stems from the ability to easily control their size, and thus their energy bandgap. While the size dependence of optical properties of nanocrystals has been extensively studied, relatively little work has been done to date to assess the impact of nanocrystal size on the electronic properties of semiconducting solids composed of nanocrystals [1]. In classical device physics, semiconductors are characterized with temperature dependent measurement techniques. Here, we apply a variety of temperature-dependent characterization techniques to systematically assess the properties of nanocrystal-based solids composed of different size-nanocrystals.
Due to their potential for low cost solar cells [2], lead sulfide (PbS) nanocrystals are investigated here. The nanocrystal synthesis and solar cell device fabrication follow the procedure described in recent work by our group [3]. For devices fabricated with each size nanocrystal, in addition to standard photovoltaic characterization under AM1.5G illumination (V_{OC}, J_{SC}, Fill Factor, and power conversion efficiency), we perform temperature dependent transient open circuit

voltage (trVoc) measurements to determine the recombination dynamics, temperature dependent IV measurements to find the reverse saturation current, and thermal admittance spectroscopy (TAS), to assess charge trapping behavior [3]. The combination of the above-mentioned temperature dependent measurement methods allows us to develop a more complete picture of the factors limiting performance of PbS nanocrystals solar cells.

[1] W. Yoon et al., *Sci. Rep.* **3,** 2225 (2013). [2] E.H. Sargent, *Adv. Mater.* **20,** 3958–3964 (2008). [3] D. Bozyigit et al., *Nano Lett.* **13,** 5284–8 (2013).

* Authors contributed equally

Sound Waves for the Handling of Droplets

Ivo Leibacher, Peter Reichert and J. Dual

Center of Mechanics, D-MAVT

The miniaturization of biological-chemical laboratory processing has evolved into the field of "droplet microfluidics" over the last decade. A main goal of this field is the handling of discrete fluid droplets, i.e. reagents, on microfluidic chips, resulting in fast and cheap "lab on a chip" devices. For these droplets, a set of unit operations is necessary for their handling, i.e. droplet fusion, sorting and storage. For such unit operations, fluid handling methods are sought. An ideal handling method would be a contact-free external force field which acts selectively on certain fluid droplets. Acoustic methods fulfill these criteria. The abstract at hand proposes a novel method for droplet handling in bulk acoustic wave (BAW) devices. Whereas bulk wave methods have formerly focused on particle handling, here we demonstrate their ability for droplet handling.
The experimental results comprise 4 unit operations: fusion, exchange of the continuous phase, sorting and storage of droplets. All of these unit operations were achieved with a BAW method and water-in-oil droplets on silicon devices. In this method, an ultrasonic standing wave is excited across a microfluidic channel of 1 mm width around 500 kHz. The setup with a simple piezoelectric transducer is well suited for miniaturization and the lab on a chip concept.
For droplet fusion, two droplets are pressed together by acoustic radiation forces, which induces their fusion. Droplet sorting was achieved at a channel bifurcation, where the droplet path can be chosen by switching the acoustic frequency. These and further methods were analyzed experimentally, numerically and analytically.
The described acoustofluidic method is believed to offer significant benefits for the handling of microfluidic droplets e.g. for biochemical research, laboratory diagnostics and drug screening applications.

Session 2: 11:00 – 12:20

Max Kory, M. Wörle, T. Weber, C. Becher and A.D. Schlüter

Polymer Chemistry, D-MATL

Gram-Scale Synthesis of Organic Two-Dimensional Polymer Crystals and Exfoliation into Nanometer-Thin Sheets

Ever since the discovery of graphene, a natural two-dimensional polymer (2DP), it has become evident that macromolecular sheets consisting of covalently bonded repeating units bear many interesting prospects for nanotechnology. Up until recently, a bottom-up preparation of such structures based on a carbon scaffold has not been achieved. Here we report that noncentrosymmetric, enantiomorphic single crystals of a simple-to-make monomer can be photochemically converted into chiral 2DP crystals on the multigram scale, and by thermal treatment also cleanly reversed back to monomer. The crystal structure of the two-dimensional polymer was elucidated by single crystal XRD which provides unequivocal structural proof of this synthetic macromolecule. The highly robust monomer crystals can be grown to sizes larger than 1mm and the 2DP crystals can be exfoliated to nanometer-thin sheets. Both monomer and polymer crystals show pronounced second-harmonic generation which makes them interesting materials for applications in the field of nonlinear optics.

Ye Tao and C.L. Degen

Spin Physics and Imaging, D-PHYS

Facile Fabrication of Single-Crystal-Diamond Nanostructures with Ultrahigh Aspect Ratio

Diamond has emerged as a unique material for a variety of applications, both because it is very robust and because it has defects with interesting properties. The shaping of diamond into suitable nanostructures, such as thin membranes, cantilevers or nanoscale sensor heads for scanning NV magnetometry, is a technological challenge that presents a major obstacle towards integrated diamond devices. In this talk, I will show how our group responds to these challenges by developing new techniques for fabricating diamond nanostructures. Examples include mechanical cantilevers as thin as 50 nm and with aspect ratios exceeding 1:2'000, and different types of diamond tips and pillars. I will also show how we can use surface chemical modifications to control the mechanical properties of the resonators, and show possible improvements to future diamond devices.

Wolfram Grüning and C. Copéret

Surface and Interfacial Chemistry, D-CHAB

C–H Activation with Iridium(I) on Bipyridine-Containing Periodic Mesoporous Organosilicas

Periodic Mesoporous Organosilicas (PMO) are hybrid organic inorganic materials with a high density of organic linkers in the walls [1–4]. For aromatic groups supramolecular ordering is observed to give crystal-like structures [5].
We describe the preparation of a new PMO containing bipyridine moieties as ligands. The material exihibits a high surface area and ordering with in the pore walls. After passivation and functionalization with $[IrCl(COD)]_2$ we obtain a material with molecularly defined iridium surface complexes.
The materials catalyze the reaction of arenes with diboranes to aryl boronic acids with identical activity and selectivity as their homogenous analogues [6].

[1] T. Asefa et al., *Nature* **402**, 867 (1999). [2] B.J. Melde et al., *Chem. Mater.* **11**, 3302 (1999). [3] S. Inagaki et al., *J. Am. Chem. Soc.* **121**, 9611 (1999). [4] F. Hoffmann and M. Fröba, *Chem. Soc. Rev.* **40**, 608 (2011). [5] S. Inagaki et al., *Nature* **416**, 304 (2002). [6] W. R. Grüning et al., *Adv. Synth. Catal.* **356**, 673 (2014). For related work see: M. Waki et al., *J. Am. Chem. Soc.* **136**, 4003 (2014).

Tommaso Delpero, A. Bergamini and P. Ermanni

Composite Materials and Adaptive Structures, D-MAVT

Adaptive Materials for Programmable Meta-materials

The peculiar macroscopic properties of meta-materials result from the interactions of their unit cells at the micro- and meso-scales, as well as from the bulk behavior of the materials they are com-posed of. In a mechanical context, the connectivity pattern of the unit cells is defined by the ability of neighboring elements to interact with one another by transmitting mechanical stresses. In this work, we experimentally demonstrate how the introduction of adaptive materials at the unit cell level allows for controlling the effective mechanical impedance distribution, and thus the overall properties, of mechanical metamaterials.
The investigated structures consist of aluminum plates with periodic arrays of cylindrical stubs and shunted piezoelectric discs, whose arrangement has been carefully designed to alter the propagation of mechanical waves in a controllable way. The effective stiffness of the shunted piezoelectric discs is shown to be able to create, shift and cancel bandgaps in the dispersion relations of the considered metamaterials.
The originality of the approach lies in the way the metamaterial properties are controlled: the modification of the dispersion properties is obtained neither by changing the bulk material properties nor the geometry of the constituting elements, but the connectivity of the crystal structure. Additionally, the energy exchange between the mechanical and the electrical domain offered by the piezoelectric material and the possibility to control it by means of simple analog circuits point to a new opportunity that the presented system offers: the development of a new class of 'programmable' materials, whose mechanical properties can be controlled via the modification of the parameters of arrays of simple electrical circuits.

MaP Award 2014: 14:00 – 15:20

Dr. Johannes Haberl

Food and Soft Materials, D-HEST

Magnetic Liquid-Crystalline Elastomers

Remotely controlled actuation with wireless sensorial feed-back is desirable for new materials to obtain fully computer-controlled actuators. Here, a light-controllable polymeric smart material is presented, in which exposure to light couples with a change in magnetic properties, allowing light signal conversion into non-volatile magnetic memory. The material can serve both as actuator and transducer and allows the monitoring of its two-way elastic shape-changes by magnetic read-out.
In order to achieve full control of the resultant magnetic anisotropy in response to external stimuli, a new liquid-crystalline elastomer (LCE) matrix is used that allows fully reversible changes in shape and physical properties at the smectic-isotropic phase transition, which enables shape-memory and can convert external stimuli into mechanical work. Tensile strength analysis and X-ray scattering experiments are combined to establish a detailed understanding of the microstructural coupling between the LCE matrix and the embedded magnetic core-shell ellipsoidal nanoparticles. Under deformation, the soft response of the nanocomposite material allows the organization of the nanoparticles to yield a permanent macroscopically anisotropic magnetic material. Independently of the particle loading, the shape-memory properties and the smectic phase of the LCEs are preserved. Detailed studies on the magnetic properties demonstrate that the collective ensemble of individual particles is responsible for the macroscopic magnetic features of the nanocomposite. The synthesized material is envisioned to be applied in the development of innovative functional objects, e.g. computer-

controlled smart clothing, sensors, signal encoding, micro-valves and robotic devices.

Dr. Martina Hitzbleck

Biosensors and Bioelectronics, D-ITET and Experimental Biosciences Group, IBM Research-Zurich

Advanced Capillary-Driven Microfluidic Chips for Diagnostic Applications

Self-driven microfluidics represent a promising concept for the development of novel diagnostic devices. Capillary-driven microfluidic chips based on hydrophilic microchannels can be used to transport liquids and to perform miniaturized immuno- and DNA assays. In view of being used as commercial diagnostic tests, these chips should meet the following requirements: (i) precise manipulation of μL-liquid volumes, (ii) integration of small amounts of reagents (ng and less), (iii) formation of a quantitative assay signal, (iv) easy handling by a user and mostly autonomous actuation of the chip, and if possible (v) low cost production/mass manufacturability. The aim of my thesis was to provide advanced control on liquids and reagents inside microfluidic chips that pave the way for performing more complex diagnostic tests while maintaining the simplicity of use. This work presents a toolbox of functional elements that can be tailored separately and combined into complex microfluidic networks to demonstrate their performance in biological assays.

Dr. Rafael Libanori

Complex Materials, D-MATL

Bioinspired Composites with Controlled Alignment and Distribution of Anisotropic Reinforcing Particles

Biological materials exhibit outstanding mechanical performance even though they are comprised of relatively weak building blocks. As the availability of chemical elements in living organisms is rather limited, these materials had to evolve intricate microstructures through natural selection processes to compensate for the use of weak components. Combining such microstructural design of biological systems with the diverse chemistry of synthetic building blocks may lead to the fabrication of bio-inspired artificial composites exhibiting remarkable mechanical properties and functionalities. In this context, this PhD thesis aimed at the development of processing routes to manufacture synthetic materials that incorporate into their microstructures one or more of the design principles found in many natural materials. We especially focused on the fabrication of bio-inspired composites presenting local mechanical properties tailored through the precise control over the orientation and spatial distribution of reinforcing platelets within polymeric matrices. Such general design principle is a hallmark of many composite materials found in biological systems, including mollusk shells, arthropods, bone, teeth and plants.

Dr. Matthias Muoth

Micro and Nanosystems, D-MAVT

Clean Integration of Single-Walled Carbon Nanotubes for Electromechanical Systems

Carbon nanotubes are especially interesting for low-power sensors. However, to fully exploit the properties of an individual single-walled carbon nanotube in an electromechanical or electronic device, contacts must be fabricated while maintaining low defect density and cleanliness of the carbon nanomaterial. Standard microfabrication approaches rely on resist-based lithography that contaminate nanotubes, leading to device instabilities such as gate hysteresis.

Here, integration of single-walled carbon nanotubes is achieved in a clean manner without harsh cleaning and while maintaining broad material compatibility for contacts. Hysteresis-free, chirality-assigned carbon nanotube transistors are integrated onto microfabricated actuators that are compatible with transmission electron microscopy (TEM) for high-resolution imaging, electron diffraction for chirality assignment, and confocal Raman spectroscopy for revealing phonon frequency shifts upon tensile strain.

Freestanding nanotubes are cleanly transferred onto pre-defined metal electrodes. Transfer enables improved control over nanotube position, orientation, number, and type. Stencil lithography is implemented by on-chip shadow masks to enable resist-free patterning of additional metal electrodes which are self-aligned, cone-shaped, and provide improved mechanical clamping. Both fabrication approaches for nanotube transistors eliminate gate hysteresis even when operated at humid ambient conditions - attributed to the absence of oxides and contaminations. A surface-selective encapsulation was established to provide passivation for contacts of gas sensors.

Mechanical straining was performed inside a TEM. Electromechanical responses of chirality-assigned, suspended nanotube transistors to uniaxial strain were recorded. As expected from theory, the strain-induced change in conductivity depends on chirality.

The clean integration strategies suppress hysteresis and reduce threshold voltage fluctuations. In combination with the demonstrated structure assignment, the fabrication approaches provide a solid platform for the evaluation of individual, high-quality carbon nanotubes as electromechanical transducers, including resonators.

Session 3: 15:50 – 16:50

Nicolas Broguiere, G. Palazzolo and M. Zenobi-Wong

Cartilage Engineering and Regeneration, D-HEST

Synthetic Extracellular Matrix for 3D Cultures of Central Neurons

Hydrogels optimized to promote neurite outgrowth of encapsulated neurons are very promising both as a tunable 3D in vitro model of neural tissue and for treating neural injuries in vivo. Synthetic hydrogels such as polyethylene glycol (PEG) are usually considered "blank" 3D matrices in which functionality can be added through bioactive molecules. PEG hydrogels have been shown to be biocompatible in the primate brain and to support 3D outgrowth of neurites from robust peripheral neuron clusters. However, PEG gels meeting the stringent requirements of 3D cultures for dissociated central neurons are still lacking. The goal of this study was to fill this gap.

We found that neurons were critically sensitive to many parameters. Best results were obtained with the Michael addition of thiol on vinylsulfone at pH 7.4. Additional nutrients and HA were required to keep the cells alive and immobile during the slow gelation (30 min - 1 h). Gels also had to be very soft (on the order of 500 Pa) but stable. Laminin or additional adhesion peptides like IKVAV, YIGSR, and RGD did not give a marked improvement in the presence of HA.

We studied direct interactions of the cells with the PEG chains by making 20 kDa 4arm-PEG-vinylsulfone tagged with tetramethylrhodamine, and could observe both the pore structure of the PEG gels and extensive intracellular PEG uptake by neurons, but not by astrocytes. These results suggest that the view of PEG as a fully inert and biocompatible material should be re-evaluated by the tissue engineering community. In optimized conditions, we obtained 75-80% viability two days after encapsulation and neurite outgrowth of the order of 1mm/live neuron in 5 days.

Dr. Kiran Chikkadi, M. Muoth, C. Roman, V. Maiwald and C. Hierold

Micro and Nanosystems, D-MAVT

Ultra-Low Power Gas Sensors Using Carbon Nanotubes

Present-day gas sensors suffer from high power consumption because they often operate at high temperatures, which requires the use of high-power heaters. As a result, they are unsuitable for low-power applications such as sensor network nodes for air quality monitoring and mobile applications. Carbon nanotubes are able to detect toxic gases such as NO_2 at ambient temperature, which makes them lucrative as ultra-low power gas sensors. However, the recovery of the sensor after exposure requires several hours at ambient conditions. In this work, we explore ultra-low power self-heating in suspended carbon nanotube gas sensors, which can operate at about 100 nW and recover at 2.9 μW. This represents the lowest operating power for any gas sensor ever reported.

Dr. Niko Münzenrieder, G. Salvatore, L. Petti, T. Kinkeldei, L. Büthe, C. Vogt, G. Cantarella and G. Tröster

Wearable Computing, D-ITET

Electronic Membrane

In the last decades silicon based semiconductor technology enabled electronic devices like computers and smart phones, these devices changed nearly all aspects of our lives. The next step to improve the user benefit will be the integration of electronic functionality into everyday objects such as textiles, smart tags, and implantable medical devices. Since most of the objects in our daily life are bendable, foldable or elastic, the integration of rigid silicon chips is not possible. Here, thin-film transistors (TFTs) are fabricated on a flexible membrane. Therefore 400 nm of water soluble polyvinyl-alcohol (PVA) and 1 μm of parylene are deposited on a Si substrate. Next, transparent bottom-gate TFTs based on Indium-Gallium-Zinc-Oxide and Indium-Tin-Oxide are fabricated using a maximum process temperature of 150°C. Subsequently the parylene membrane is released by dissolving the PVA sacrificial layer in water. Afterwards the free-standing electronic membrane can be transferred to nearly any kind of flexible or curved surface. The TFTs exhibit a threshold voltage around 3.4 V, a mobility of ≈26 cm^2/Vs, and an on/off ratio $>10^6$ even when they are transferred to surfaces like living tissue or wrapped around a human hair of radius ≈50 μm. This combination of high electrical performance, transparency and mechanical flexibility enables new applications for electronics, which is finally demonstrated by an electronic contact lens.

POSTER PRESENTATIONS

Name	Poster Title	Affiliation	Poster No.	
Andina Diana	Fluorescent Probes for Specific Detection of Reactive Oxygen Species in Inflamed Intestine	Drug Formulation & Delivery, D-CHAB	**14**	**A**
Becher Carsten	Nanocapacitors by Strain-Induced Defect-Polarization Coupling in $SrMnO_3$ Films	Multifunctional Ferroic Materials, D-MATL	**28**	**B**
Bernoulli Daniel	Influence of the Film Thickness on Fragmentation, Adhesive Failure and Contact Damage of Diamond-Like Carbon (DLC) Coated Titanium Substrates	Nanometallurgy, D-MATL	**36**	**A**
Boenzli Eva	Controlled Fusion of Giant Unilamellar Vesicles Using Viral Fusogenic Peptides	Bioanalytics Group, D-CHAB	**1**	**A**
Böni Lukas	Rheology of Hagfish Slime - a Marine Biopolymer	Food Process Engineering, D-HEST	**19**	**C**
Bran Anleu Paula	High Performance Fiber Reinforced Lightweight Concrete	Physical Chemistry of Building Materials, D-BAUG	**50**	**C**
Brenner Oliver	Air Entrainment Simulation of Tube-Enclosed Flame Aerosol Synthesis of Nanoparticles by Computational Fluid Dynamics	Particle Technology Laboratory, D-MAVT	**43**	**C**
Büchel Robert	Effect of Ba and K in Rh/Al_2O_3 Catalysts for CO_2 Hydrogenation	Particle Technology Laboratory, D-MAVT	**44**	**B**
Bzdusek Tomas	Realization of a Topological Semimetal in a Crystal with Preserved Time-Reversal Symmetry	Strongly Correlated Electrons, D-PHYS	**60**	**C**
Cantarella Giuseppe	A PDMS-Based Strain Sensor	Wearable Computing, D-ITET	**66**	**B**
Caruso Francesco	Predicting the Future of Salt-Weathered Stone	Physical Chemistry of Building Materials, D-BAUG	**51**	**B**
Cremmel Clément V.M.	From Nano to Micro, a Challenge in Bridging Scales	Surface Science and Technology, D-MATL	**62**	**C**
Dasargyri Athanasia	Exploring Lymph Node Metastatic Dissemination Using Fluorescent Particles	Drug Formulation & Delivery, D-CHAB	**15**	**B**
de Lange Victoria	The FoRe Microarray: A Simple and Inexpensive Technique for Multiplexed Protein Detection in Minute Clinical Samples	Biosensors and Bioelectronics, D-ITET	**5**	**A**

Döring Valentin	Clean and Efficient Transfer of Carbon Nanotubes for Device Fabrication	Micro and Nanosystems, D-MAVT	**25**	**A**
Durrer Lukas	Pulsed Bi_2Te_3 Plating for Large Scale Production of Thermoelectric Converters	Micro and Nanosystems, D-MAVT	**26**	**B**
Dymkowski Krzysztof	Strain-Induced Metal-Insulator Transitions in d^1 Perovskites within DFT+DMFT	Materials Theory, D-MATL	**22**	**C**
Etter Sarah	Limiting Mechanism for Critical Current in Topologically Frustrated Josephson Junctions in Sr_2RuO_4	Theoretical Physics, D-PHYS	**64**	**A**
Ezbiri Miriam	Thermochemical Separation of Oxygen from Inert Gas via Perovskite-Based Redox Cycles Utilizing Solar Waste Heat	Renewable Energy Carriers, D-MAVT	**58**	**B**
Fedorova Natalya	Magnetic Properties of Multiferroic $TbMnO_3$	Materials Theory, D-MATL	**23**	**A**
Gauthier Nicolas	Magnetic Excitations of J_1-J_2 Zigzag Chains in $SrDy_2O_4$ Frustrated Magnet	Laboratory of Developments and Methods, D-PHYS, Paul Scherrer Institute	**21**	**B**
Gong Yuhui	Reversible and Tunable PEGylation at Arginine Residues	Drug Formulation & Delivery, D-CHAB	**16**	**C**
Goudeli Eirini	Coagulation of Fractal-Like Aerosols in the Transition Regime	Particle Technology Laboratory, D-MAVT	**45**	**C**
Gröhn Arto	Scale-Up of Nanoparticle Synthesis by Flame Spray Pyrolysis: The High Temperature Particle Residence Time	Particle Technology Laboratory, D-MAVT	**46**	**A**
Hassani Mohammad Masoud	Investigation of Delamination Process in Adhesively Bonded Hardwood Elements under Changing Environmental Conditions	Computational Physics of Engineering Materials, D-BAUG	**12**	**A**
Heiligtag Florian	Nanoparticle-Based Multicomponent Aerogel Monoliths	Multifunctional Materials, D-MATL	**32**	**A**
Héroguel Florent	Controlled Growth and Interfaces of Supported Iridium Nanoparticles via Surface Organometallic Chemistry	Surface and Interfacial Chemistry, D-CHAB	**61**	**A**
Hirsch Ofer	In-Situ X-Ray Absorption and Emission Spectroscopy Study of the Interaction between CO_2 and Lanthanum-Oxycarbonate Nanoparticles	Multifunctional Materials, D-MATL	**33**	**B**
Junesch Juliane	Nanowells in Insulator-Metal Double Layers for "Spatial" Plasmonic Sensing	Biosensors and Bioelectronics, D-ITET	**6**	**B**
Kakeru Fujiwara	Visible-Light Active Black TiO_2-Ag/TiO_x Particles	Particle Technology Laboratory, D-MAVT	**47**	**B**

Kandemir Ayse Cagil	Polymer and Polymer Nanocomposite Patterning by Dip Pen Nanolithography	Nanometallurgy, D-MATL	**37**	**B**
Kesti Matti	A Novel Bioink Based on Thermo- and Photo-Triggered Tandem Gelation for Cartilage Engineering	Cartilage Engineering and Regeneration, D-HEST	**9**	**B**
Koirala Rajesh	Oxidative Coupling of Methane on Flame-Made Mn-Na_2WO_4/SiO_2: Influence of Catalyst Composition and Reaction Conditions	Particle Technology Laboratory, D-MAVT	**48**	**C**
Kreiliger Thomas	Towards Germanium X-Ray Detector Monolithically Integrated on Silicon CMOS	Physics of New Materials, D-PHYS	**55**	**A**
Küchler Andreas	Enzyme Immobilization with a Dendronized Polymer for Surface-Localized Cascade Reactions	Polymer Chemistry, D-MATL	**56**	**B**
Leo Naëmi	Flipping Ferroelectric Domains with Magnetic Fields	Multifunctional Ferroic Materials, D-MATL	**29**	**A**
Lilienblum Martin	Exotic Ferroelectric Order in Multiferroic h-$YMnO_3$	Multifunctional Ferroic Materials, D-MATL	**30**	**B**
Liu Wei	Optimizing the Performance of Substrate-Bound CNFETs by Utilizing an Alumina Protective Layer	Micro and Nanosystems, D-MAVT	**27**	**C**
Lloret Ena	Smart Dynamic Casting: A Robotic Fabrication of Complex Concrete Structures	Institute of Building Materials and Architecture and Digital Fabrication, D-BAUG	**20**	**A**
Luo Alan	Multiscale Modelling of the Rheology of Complex Interfaces	Polymer Physics, D-MATL	**57**	**C**
Ma Huan	Ion Beam Induced Selective Grain Growth and Texturing in Tungsten Thin Films	Nanometallurgy, D-MATL	**38**	**C**
Marchon Delphine	Impact of Polycarboxylate Superplasticizer on Polyphased Clinker Hydration	Physical Chemistry of Building Materials, D-BAUG	**52**	**C**
Martiel Isabelle	A Reverse Micellar Mesophase of Face-Centered Cubic Fm3m Symmetry in Phosphatidylcholine/Water/Organic Solvent Ternary Systems	Food and Soft Materials, D-HEST	**17**	**A**
Mathis Christian	A Novel Setup for Measuring Solvent Permeability in Lubricating Polymer-Brush Coatings	Surface Science and Technology, D-MATL	**63**	**B**
Mettler Linus	Monitoring and Predicting the Strength Evolution of Fiber Reinforced SCC During Early Hydration	Computational Physics of Engineering Materials, D-BAUG	**13**	**C**

Muff Daniel	Mechanical Properties of Broad-Band Bragg Reflector Coatings for Dental Implants	Nanometallurgy, D-MATL	**39**	**A**
Pecnik Christina	Optical Properties and Durability of Dental Coatings	Nanometallurgy, D-MATL	**40**	**B**
Raemy Christian	Simulation of the Evolution of the Yield Locus of Deep Drawing Steel by Means of Crystal Plasticity	Virtual Manufacturing, D-MAVT	**65**	**C**
Reichert Peter & Leibacher Ivo	Sound Waves for the Handling of Droplets	Center of Mechanics, D-MAVT	**10**	**C**
Röthlisberger André	Finite Element Approach for Gas Flow Modelling in the Early Arcing Stage	Nanometallurgy, D-MATL	**41**	**C**
Sangiorgio Boris	Superconductivity and Dipole Emergence in Lead Chalcogenides	Materials Theory, D-MATL	**24**	**B**
Schaab Jakob	Tuning the Electronic Transport Behavior at Functional Ferroelectric Domain Walls	Multifunctional Ferroic Materials, D-MATL	**31**	**C**
Segmehl Jana	Copper Coating of Wood Structures	Wood Materials Science, D-BAUG	**68**	**C**
Sommer Marianne	Inverse-Opal Scaffolds Templated by Porogens Made by Microfluidics	Complex Materials, D-MATL	**11**	**B**
Staniuk Malwina	Puzzling Mechanism Behind a Simple Synthesis of Cobalt and Cobalt Oxide Nanoparticles: In Situ Synchrotron X-Ray Absorption and Diffraction Studies	Multifunctional Materials, D-MATL	**34**	**C**
Starsich Fabian	Photothermal Killing of Cancer Cells by the Controlled Plasmonic Coupling of Silica-Coated Au/Fe_2O_3 Nanoaggregates	Particle Technology Laboratory, D-MAVT	**49**	**A**
Stauffer Flurin	Conductive Elastomer Based on Silver Nanowire Networks Embedded in Silicone	Biosensors and Bioelectronics, D-ITET	**7**	**C**
Stratz Simone	A Microfluidic Device for Proteomic Analysis of Single *E. coli* Bacteria	Bioanalytics Group, D-CHAB	**2**	**B**
Sun Wenjie	Controlling Enzyme Activity and Kinetics by Physical Nano-Confinement	Food and Soft Materials, D-HEST	**18**	**B**
Suraneni Prannoy	Filling in the Gaps of Alite Hydration	Physical Chemistry of Building Materials, D-BAUG	**53**	**A**
Tanno Alexander	Triggered Surface-Mediated Neurotransmitter Delivery to Neurons	Biosensors and Bioelectronics, D-ITET	**8**	**A**
Tao Ye	Rejuvenation of Silicon Nanomechanical Resonators	Spin Physics and Imaging, D-PHYS	**59**	**A**

Verboket Pascal Emilio	A Microfluidic ICP-MS Sample Introduction System for Cell and Nanoparticle Analysis	Bioanalytics Group, D-CHAB	**3**	**C**
Vogt Christian	Micro Optical Bench for Textile Integrated MRI Data Links	Wearable Computing, D-ITET	**67**	**A**
Walser Jochen	Cell Migration and Adhesion on Electrospun Polycaprolactone Scaffolds	Biomechanics, D-HEST	**4**	**B**
Wangler Timothy	Clay Swelling in Anhydritic Claystones	Physical Chemistry of Building Materials, D-BAUG	**54**	**C**
Yazdani Nuri	Charge Transport Kinetics in PbS Nanocrystal-Based Solar Cells	Nanoelectronics, D-ITET	**35**	**B**
Zou Yu	Size-Dependent Plasticity in Ionic Crystal Systems: The Influence of Temperature, Orientation and Doping Level	Nanometallurgy, D-MATL	**42**	**A**

ABSTRACTS OF POSTERS

1-A Controlled Fusion of Giant Unilamellar Vesicles Using Viral Fusogenic Peptides

Eva Boenzli, M. Hadorn, P.E. Verboket and P.S. Dittrich

Bioanalytics Group, D-CHAB

Membrane fusion is a complex mechanism involved in various cellular processes. Viral infections of host cells also require fusion of membranes for virus entry, a process that is triggered by low pH and viral surface proteins. Fusion peptides (FPs) derived from the surface glycoprotein of Influenzavirus can be used to study the fusion of artificial membranes. However, investigations of fusion events are laborious and ineffective, and the reproducibility is poor. Here, we present a microfluidic platform designed to spatially and temporally control the fusion of giant unilamellar vesicles (GUVs) using Influenzavirus FPs, which are activated by a pH change. Our microfluidic chip was designed to trap GUVs, to bring them into close contact, and to completely isolate them from the environment. Phospholipid GUVs were produced and mixed with viral FPs. On the chip, membrane fusion was induced by a pH trigger and monitored with a high-speed camera. With our system that allows the controlled fusion of two or multiple vesicles trapped on the chip, exact analyses become feasible, e.g. of the membrane fusion mechanism. Our results revealed that vesicles follow a defined fusion process; they undergo aggregation followed by a zipper-like formation of a hemifusion area. After several seconds, complete fusion is induced represented by a fusion pore. As proof of complete fusion, we monitored content mixing and we did analyses on volume and surface area before, during and after fusion. In summary, we have established a system that allows studying fusion in an effective, controllable, and high-throughput manner, representing a perfect tool for deeper analyses of the theoretical membrane fusion mechanism.

2-B A Microfluidic Device for Proteomic Analysis of Single *E. coli* Bacteria

Simone Stratz, K. Eyer, F. Kurth and P.S. Dittrich

Bioanalytics Group, D-CHAB

Bacteria of a clonal microbial culture can exhibit significant phenotypic heterogeneity. This cellular diversity predominantly originates from noisy gene expression and is intended to enhance fast adaption of a microbial population to chancing environmental conditions. As a consequence, these cell-to-cell differences also facilitate the emergence of antibiotic resistant microorganisms, like for example potential harmful hospital pathogens. The study of phenotypic diversity as well as the regulating control mechanisms behind requires analysis of single cells. Recently, several promising microfluidic systems for cell studies have been developed, where most of them were optimized for mammalian cells. Platforms capable of handling considerably smaller microorganisms with sizes in the range of sub micrometers to a few micrometers, hence with volumes of about 1000 times smaller than average mammalian cells are still rarely found. Here, we present a microfluidic platform suitable for capture, isolation and proteomic analysis of single *E. coli* bacteria. Main feature of the device is a set of 60 microchambers each providing centrally positioned micrometer sized structures for mechanical bacteria trapping surrounded by a ring-shaped valve which when actuated isolates the trapped bacterium in a volume of 72 pL. Subsequent immunoassay based analysis of the cell lysates of single *E. coli* enabled selective and sensitive quantification of the intracellular enzyme beta-galactosidase which serves as an indicator for bacteria adaptation to changes of the carbon source in the nutrient medium. As proof-of-concept study we determined the beta-galactosidase levels of single *E. coli* cultured under two different growth conditions with a limit of detection of 100 enzymes. The strong variations we observed within the ß-galactosidase levels of individual bacteria motivate the usage of the microfluidic device in future proteomics and metabolomics studies of isogenic bacterial populations.

3-C A Microfluidic ICP-MS Sample Introduction System for Cell and Nanoparticle Analysis

Pascal Emilio Verboket, O. Borovinskaya, N. Meyer, D. Günther and P.S. Dittrich

Bioanalytics Group, D-CHAB

Today, inductively coupled plasma mass spectrometry (ICP-MS) is an important tool for highly sensitive elemental analysis of single nanoparticles or rare-earth isotope labeled cells. This type of measurement requires a discrete sample introduction system with high transport efficiency. However, commercially available droplet injection modules are expensive, suffer from a narrow droplet size range, are prone to clogging and difficult to clean. To overcome these drawbacks a robust, flexible, low

cost and low-maintenance sample introduction system for measurements of nanoparticles and single cells by ICP-MS is of interest.
We present a novel method to interface a continuous-flow droplet microfluidic based system with ICP-MS, which enables sensitive elemental analysis of the content of picoliter size droplets containing cells or nanoparticles. Our system is build around a disposable Polydimethylsiloxane liquid-assisted droplet ejection (LADE) chip, which generates aqueous droplets and ejects them in to the ICP-MS. It can measure samples as small as 1 μl and opens the possibility to easily integrate further sample pretreatment steps into the microfluidic device.
In this study, the interface was used for the quantification of the iron content of red blood cells. Additionally, the optimization of the system and its potential for the measurements of nanoparticles will be discussed.
In summary, we have demonstrated a droplet-based microfluidic chip as sample introduction system for ICP-MS. Our system is disposable, easy to use and robust. We have shown its use for single cell analysis.

4-B Cell Migration and Adhesion on Electrospun Polycaprolactone Scaffolds

Jochen Walser and S.J. Ferguson

Biomechanics, D-HEST

Introduction: As electrospun Polycaprolactone (PCL) scaffolds show great potential for various tissue engineering applications, the aim of this study was to evaluate cell adhesion, migration and proliferation on these scaffolds.
Materials and Methods: 210 punches from random aligned electrospun PCL scaffolds were used for one 7-day cell proliferation (CP), two 24-hour cell adhesion (CA-1 and CA-2) and two 48-hour cell migration (CM-1 and CM-2) experiments. Three different cell types, a 3T3 cell line (3T3), native bovine articular chondrocytes (barc) and native bovine auricular chondrocytes (bauc) were used for each experiment. CP and CA-1 was evaluated using a MTT test, while for CA-2 and CM-1 confocal microscopy with DAPI and phalloidin staining as well as CMFDA cell tracker has been used. Confocal image data was analysed using ImageJ. CM-2 was evaluated by SEM imaging after a dehydration and gold sputter coating procedure.
Results: While barc showed the best cell adhesion in both CA-1 and CA-2, they also displayed the slowest proliferation rate in CP. Nevertheless CP revealed rapid cell proliferation for all three cell types with 3T3 cell showing the strongest increase in metabolic activity. The number of adherend cells increased for all cell types and sampling points in both CA experiments with the exception of 3T3-CA-2. CM-1 using phalloidin staining shows a nice cell attachment and spreading as well as a clear alignment of stress fibres of the cytoskeleton to the spun PCL fibres.

5-A The FoRe Microarray: A Simple and Inexpensive Technique for Multiplexed Protein Detection in Minute Clinical Samples

Victoria de Lange and J. Vörös

Biosensors and Bioelectronics, D-ITET

We developed the FoRe (forward and reverse) microarray to exploit the advantages and eliminate several drawbacks of traditional protein microarrays (*i.e.* large sample volumes, protein loss, and cross-reactivity between detection antibodies) [1]. The innovative three-dimensional (3D) design is a simple, low-cost, and highly customisable vertical flow device, designed to analyse several 1 µl samples in parallel for multiple proteins. The FoRe microarray has broad applications in research; for example, in analysing cell lysate in drug response studies or pricks of blood from small animal studies.
The concept of the FoRe microarray is "stack-and-separate." Capture antibodies are passively adsorbed to nitrocellulose membranes, which are then stacked to form a multiplexed affinity column. The device is easily customisable—any combination of test sites can be assembled. As the sample passes through the stack, target proteins are specifically adsorbed to the different layers. This eliminates protein loss by simultaneously sorting and spotting the sample. To analyse several samples in parallel, we introduced hydrophobic wax barriers around the antibody-loaded spots on each layer. Wax printing is a rapid and inexpensive technique, which requires only a standard office printer [2]. When stacked and aligned, the patterned nitrocellulose creates a microarray of 25 multiplexed affinity columns.
We demonstrated multiplexed detection of rabbit and mouse IgG in buffer spiked with bovine serum albumin (BSA). The device is also compatible with plasma, achieving a sensitivity of 15 pM for a sandwich assay detecting mouse IgG.In spite of its simplicity, the system is sensitive enough to detect clinically relevant protein concentrations in complex samples.

[1] V. de Lange and J. Vörös, *Anal. Chem.*, **86**, 4209–4216 (2014). [2] Y. Lu et al., *Anal. Chem.*, **82**, 329–335 (2010).

6-B Nanowells in Insulator-Metal Double Layers for "Spatial" Plasmonic Sensing

Juliane Junesch, A. Dahlin and J. Vörös

Biosensors and Bioelectronics, D-ITET

7-C Conductive Elastomer Based on Silver Nanowire Networks Embedded in Silicone

Flurin Stauffer, V. Martinez, M. Adagunodo, J. Vörös and A. Larmagnac

Biosensors and Bioelectronics, D-ITET

Conductive elastomers have interesting properties for use in diverse conformal devices for monitoring, diagnosing and therapeutic purposes in medicine, e.g. human motion sensors as well as stretchable multielectrode arrays (MEAs) for electrical stimulation. Our research focuses on producing patterned structures of conductive elastomers that remain conductive over strains as high as 50% and that are biocompatible, mechanically robust and stable over several months as implant material in vivo. We investigate the electrical response under mechanical stress and the stability in saline of patterned silver nanowire networks embedded in PDMS. We show promising preliminary results towards the development of miniaturized stretchable MEAs and strain sensors with high gauge factor over high deformation.

8-A Triggered Surface-Mediated Neurotransmitter Delivery to Neurons

Alexander Tanno, N. Graf, H. Dermutz, V. Delange, Y. Beldengrün, T. Zambelli and J. Vörös

Biosensors and Bioelectronics, D-ITET

Functionalized surfaces, that allow for the release of a substance, controlled in dosage, spatial distribution and time, have the potential to contribute to improvements in tissue healing after implantations, local drug delivery and drug screening.
The platform is based on an ITO substrate that is coated with a sandwich structure of polyelectrolyte multilayer/liposomes/polyelectrolyte multilayer where the liposomes are previously loaded with a substance, e.g. a dye or a neurotransmitter, like in the actual case. Cells can be seeded on top of the platform. The drug delivery mechanism is triggered by the application of a current. This current induces water electrolysis and hence lowered local pH in the immediate vicinity of the electrode. The polyelectrolyte multilayers were designed to resist such a pH change, while the liposome membrane is intentionally made of pH-sensitive phospholipids. If the pH is lowered, the lipids are protonated, which induces a shape change of these lipids.
Consequently, the loaded vesicles cargo diffuses out of the vesicles, driven by the existing concentration gradient. To demonstrate the process, we chose a cargo that once is released from the vesicles, labels the cells, which were seeded on top of the structure.
The described release platform is now combined with neurons grown on filter paper. By stacking multiple layers of paper on top of each other, a three dimensional neuronal network can be realized. Additionally, the paper can easily be patterned. The goal of the actual project is the realization of an artificial synapse. In order to do so, neurons grown on paper are stacked upside down on the previously described release platform, which is loaded with a neurotransmitter. This neurotransmitter is then released electrochemically to the neurons, which triggers an action potential.

9-B A Novel Bioink Based on Thermo- and Photo-Triggered Tandem Gelation for Cartilage Engineering

Matti Kesti, M. Müller, J. Becher, M. Schnabelrauch, M. D'Este, D. Eglin and M. Zenobi-Wong

Cartilage Engineering and Regeneration, D-HEST

Introduction: Bioprinters for rapid prototyping purposes are well developed; however, there is still a lack of suitable biologically relevant printing materials, so called bioinks. The ideal bioink for extrusion printing should be initially liquid to allow for mixing with cells or peptides and show a flow behavior suitable for the extrusion process. The final construct should be a stable, irreversibly crosslinked hydrogel with similar mechanical properties to the surrounding tissue. We have developed a bioink suitable for bioprinting with high cell viability. This bioink utilizes a tandem gelation process with a transient initial crosslinker and photocrosslinked biopolymer forming an interpenetrating network.
Methods: Thermoresponsive hyaluronan grafted Poly(*N*-isopropylacrylamide) (HA-pNIPAAM) was mixed with the UV crosslinkable methacrylated hyaluronan. Cell encapsulated scaffolds were printed with a 300 μm needle on a heated substrate (37°C) and after 10 s UV exposure of each layer a final thickness of 2.8 mm was achieved. Elution of the reversibly crosslinked, transient HA-pNIPAAM structure was performed in PBS at 4°C for 30 minutes. Chondrocyte viability was assessed with a MTS assay and live/dead assay after 4 days.
Results: The bioprinted structures were stable after photocrosslinking with good resolution. After the HA-pNIPAAM was eluted, the structures maintained their shape and became transparent. In the MTS assay the printed scaffold viability was 91.6% of the positive control.

Discussion & Conclusions: In order to create a more open, porous network where nutrients and gas exchange can take place, HA-pNIPAAM was intentionally removed from the hydrogels. This biocompatible bioink utilizes a tandem gelation process with a transient initial crosslinker to overcome the rheological limitations of pure biopolymer printing. This method can be used to facilitate 3D printing of biopolymer solutions which areotherwise not printable, thereby greatly expanding the range of bioink possibilities.

10-C Sound Waves for the Handling of Droplets

Peter Reichert, Ivo Leibacher and J. Dual

Center of Mechanics, D-MAVT

The miniaturization of biological-chemical laboratory processing has evolved into the field of "droplet microfluidics" over the last decade. A main goal of this field is the handling of discrete fluid droplets, i.e. reagents, on microfluidic chips, resulting in fast and cheap "lab on a chip" devices.
For these droplets, a set of unit operations is necessary for their handling, i.e. droplet fusion, sorting and storage. For such unit operations, fluid handling methods are sought. An ideal handling method would be a contact-free external force field which acts selectively on certain fluid droplets. Acoustic methods fulfill these criteria. The abstract at hand proposes a novel method for droplet handling in bulk acoustic wave (BAW) devices. Whereas bulk wave methods have formerly focused on particle handling, here we demonstrate their ability for droplet handling.
The experimental results comprise 4 unit operations: fusion, exchange of the continuous phase, sorting and storage of droplets. All of these unit operations were achieved with a BAW method and water-in-oil droplets on silicon devices. In this method, an ultrasonic standing wave is excited across a microfluidic channel of 1 mm width around 500 kHz. The setup with a simple piezoelectric trans-ducer is well suited for miniaturization and the lab on a chip concept.
For droplet fusion, two droplets are pressed together by acoustic radiation forces, which induces their fusion. Droplet sorting was achieved at a channel bifurcation, where the droplet path can be chosen by switching the acoustic frequency. These and further methods were analyzed experimentally, numerically and analytically.
The described acoustofluidic method is believed to offer significant benefits for the handling of microfluidic droplets e.g. for biochemical research, laboratory diagnostics and drug screening applications.

11-B Inverse-Opal Scaffolds Templated by Porogens Made by Microfluidics

Marianne Sommer, S. Hofmann and A.R. Studart

Complex Materials, D-MATL

Scaffolds with poorly controlled porous architecture may cause a wide variety of cell responses depending on the actual local surrounding of each single cell. Inverse-opal structured scaffolds exhibiting monodisperse and close-packed porosity offer a more homogeneous environment to cells and might thus lead to a more homogeneous or even predictable cell behavior throughout the scaffold. Such scaffolds can be produced using the porogen-leaching method. Both monodisperse particles and droplets can be made in sufficient quantities to template the pores of such scaffolds. We show that infiltrating pre-necked closely packed polymer particles generated by microfluidics with a silk fibroin solution and subsequent dissolution of the particles yields scaffolds with an inverse opal structure with biocompatible silk walls of tunable crystallinity. As an alternative route, oil droplets were directly generated in a concentrated aqueous nanoparticle suspension and stabilized with poly(vinyl alcohol) to create and inverse opal structure with open porosity upon evaporation of the solvents. By mixing a ready-made oil-in-water emulsion with a suspension of particles it is also possible to extend this method to microparticles that would otherwise lead to clogging in the microfluidic devices. Important Parameters such as pore size, interconnection size as well as surface roughness and chemistry can be deliberately tuned in these systems. Such level of control over the structure and chemistry of macroporous materials is currently being explored for the fabrication of a range of tailor-made organic and inorganic scaffolds for tissue regeneration.

12-A Investigation of Delamination Process in Adhesively Bonded Hardwood Elements under Changing Environmental Conditions

Mohammad Masoud Hassani, S. Ammann, F.K. Wittel, P. Niemz and H.J. Herrmann

Computational Physics of Engineering Materials, D-BAUG

Application of engineered wood, especially in the form of glued-laminated timbers has increased significantly. However, the strong hygric dependence of basically all mechanical properties renders many innovative ideas futile. The tendency of hardwood for higher moisture sorption and swelling coefficients lead to significant residual stresses in glued-laminated configurations, cross-laminated patterns in particular. These stress fields cause initiation and evolution of cracks in the bond-lines

resulting in: interfacial de-bonding, loss of structural integrity, and reduction of load-carrying capacity. In addition, long-term creep and mechano-sorption under changing environmental conditions lead to loss of stiffness and can amplify delamination growth over the lifetime of a structure even after decades.
In this study we investigate the delamination process of adhesively bonded hardwood (European beech) elements subjected to changing climatic conditions. Since up to now, a comprehensive moisture-dependent rheological model comprising all possibly emerging deformation mechanisms was missing, a 3D orthotropic elasto-plastic, visco-elastic, mechano-sorptive material model for wood, with all material constants being defined as a function of moisture content, was developed. Apart from the solid wood adherends, adhesive layer also plays a crucial role in the generation and distribution of the interfacial stresses. To obtain a realistic assessment on the mechanical performance of the adhesive layer and a detailed look at the interfacial stress distributions, a generic constitutive model including all potentially activated deformation modes, namely elastic, plastic, and visco-elastic creep was developed. The corresponding numerical integration approaches, with additive decomposition of the total strain are implemented within the ABAQUS FEM environment by means of user subroutine UMAT.
To predict the true stress state, we perform a history dependent sequential moisture-stress analysis using the developed material models for both wood substrate and adhesive layer. Prediction of the delamination process is founded on the fracture mechanical properties of the adhesive bond-line, measured under different levels of moisture content and application of the cohesive interface elements.

13-C Monitoring and Predicting the Strength Evolution of Fiber Reinforced SCC During Early Hydration

Linus Mettler, F.K. Wittel and H.J. Herrmann

Computational Physics of Engineering Materials, D-BAUG

The research outlined in this poster is conducted in the context of a multidiciplinary project, "Smart Dynamic Casting", where a self-consolidating concrete is shaped into a desired geometry by means of an industrial robot carrying a flexible mold. The formwork is significantly smaller than the structures produced and the material leaves the mold during the ongoing early hydration process, while it is still deformable (or "wet") and yet able to provide the strength necessary to sustain its own weight.
The thixotropic nature of the material poses a major challenge to the process, because the structural breakdown induced by the moving mold may lead locally to a sudden liquefaction and to collapse of the structure. The tradeoff between deformability and strength during hydration restricts the time for shaping to only a few minutes. It is crucial to precisely predict the mechanical and rheological properties of the material during the early phase of its transition from a complex yield stress fluid to a solid material. This challenge is tackled by a combined experimental/numerical approach, where on-line penetrometer measurements are used to adopt numerical prediction for controlling the overall process.

14-A Fluorescent Probes for Specific Detection of Reactive Oxygen Species in Inflamed Intestine

Diana Andina, D. Brambilla*, J.-C. Leroux and P. Luciani

Drug Formulation & Delivery, D-CHAB

The correlation between oxidative stress and progression of intestinal inflammation has not yet been unequivocally established. A diagnostic tool aimed at selectively and quantitatively highlighting areas rich in reactive oxygen species (ROS) in the gastrointestinal tract can add new insights to this topic.
A promising approach to produce versatile ROS-specific fluorescence contrast agents is to reduce cyanine dyes to hydrocyanines. Coupling of this fluorophore to a polymeric moiety (*e.g.* poly-ethylene glycol, PEG) allows to modulate important characteristics such as cell uptake.
The intracellular probe HCy5 was obtained by reducing Cy5 with excess $NaBH_4$. The extracellular PEG-derivative PEG-HCy5 was synthesized by coupling a PEG-NH_2 to a Cy5-NHS [2], and subsequently by reducing the PEG-dye conjugate. Cellular uptake in Caco-2 monolayers was investigated by fluorescence activating cell sorting and proven to be negligible for the PEG-conjugated fluorophore indicating the PEG-derivative can be used to exclusively detect extracellular ROS.
Hydroxyl and superoxideradicals were generated *in situ,* and detected fluorimetrically with the newly synthesized probes in a highly specific manner. Applying physical stress to differentiated Caco-2 monolayers induced ROS production and partial fluorescence recovery of the hydrocyanine in a time-dependent fashion.
These preliminary results show that both the PEG-HCy5 conjugate and the HCy5 derivative can be used to detect ROS in cell-free assays and in living cells. Furthermore, the negligible cell uptake of the PEG-conjugate suggests it as a good candidate for extracellular ROS detection.

* D. Brambilla gratefully acknowledges support from the ETH Zurich Fellowship (2012-01).

15-B Exploring Lymph Node Metastatic Dissemination Using Fluorescent Particles

Athanasia Dasargyri, P. Hervella, A. Christiansen, S. Proulx, M. Detmar and J.-C. Leroux

Drug Formulation & Delivery, D-CHAB

Objective: Although both lymphatic and blood vessels have been shown to play a role in metastatic dissemination, the relative significance of each vascular system for the development of distant organ metastases remains controversial. This project aims to develop an *in vivo* fluorescence approach to characterize the importance of lymphatic metastasis to cancer dissemination. The experimental strategy aimed to design fluorescently-labeled, non-biodegradable polymeric particles able to target metastatic cells within the lymph node (LN). The tumor-selective engulfment of labeled particles in the LNs will allow the tracking of the metastatic cells *in vivo* as they traffic to distal organs.
Methods: 1 μm fluorescently-labeled polystyrene particles were PEGylated and functionalized with anisamide, a small organic molecule reported to target the Sigma-1 receptor. The expression of Sigma-1 receptor on cancer cells would thereby enable tumor-selective particle uptake. The *in vitro* internalization of the functionalized particles by B16F10 murine melanoma cells was evaluated by flow cytometry and confocal microscopy. Silencing of the Sigma-1 receptor, followed by *in vitro* uptake experiments, was performed to assess the involvement of this receptor in the internalization process.
Results: The surface functionalization of the particles was confirmed by the alteration of the surface charge. Particle uptake studies on B16F10 cells showed enhanced internalization of the anisamide-functionalized particles. Sigma-1 receptor silencing on B16F10 cells did not alter the uptake of the particles, suggesting that the internalization is not mediated by this receptor.
Conclusions: Tumor-specific labelingparticles were prepared. Although the role of the Sigma-1 receptor in the internalization process could not be proven, the tumor selective uptake of particles enables their use in *in vivo* tumor cell tracking studies. Sentinel intranodal particle injection in mice bearing B16F10 tumors, and subsequent assessment of cells within metastatic sites will reveal involvement of the sentinel lymph node in the metastatic process.
Acknowledgements: This project is financially supported by Krebsliga Schweiz (KFS-2821-08-2011).

16-C Reversible and Tunable PEGylation at Arginine Residues

Yuhui Gong, J.-C. Leroux and M.A. Gauthier

Drug Formulation & Delivery, D-CHAB

Conjugating methoxy poly(ethylene glycol) (mPEG) to proteins (PEGylation), has been exploited as an elegant solution to prevent fast recognition and high overall clearance rate by immune system. The "tunable" release of native and fully bioactive proteins from protein-polymer conjugate system (rPEGylation) attracts increased research interest. Further expansion of the possibilities for rPEGylation at different amino acid residues is desperately required.
Phenylglyoxal (PGO), an aromatic α-oxo-aldehyde, has shown the great selectivity when combined with arginine residues in a pH-dependent manner. The PGO–arginine complex is known to be labile that could permit the reversible PEGylation at arginine, a residue for which rPEGylation has not yet been reported. Herein, a platform for selective and reversible modification of arginine residues with PGO was developed based on the reaction of guanidinium group in arginie residues with α-oxo-aldehyde.
A series of PGO-PEG derivatives with different functional groups (Mw ≈ 570 g/mol) were synthesized through the oxidation with SeO_2. Owing to PGO group, the derivatives are expected to reactwith peptide containingarginine residue. To correlate the electrostatic microenvironments with the stability of PGO-arginine adducts, several short peptides with variable charges surrounding the central arginine have been modified onto PGO-PEG derivatives, such as EEREEW, GEREGW, GGRGGW, GKRKGW, KKRKKW(E: Glutamic acid, R: Arginine, G: Glycine, K: Lysine, W: tryptophan). Differentreaction rates and mechanisms were observed in the kinetic studies of the modification of different peptides with PGO-PEG derivatives. The half-life time of each reaction were calculated and compared. Future work will focus on evaluating the rate of release of the native peptide under physiological conditions.

17-A A Reverse Micellar Mesophase of Face-Centered Cubic Fm3m Symmetry in Phosphatidylcholine/Water/Organic Solvent Ternary Systems

Isabelle Martiel, L. Sagalowicz and R. Mezzenga

Food and Soft Materials, D-HEST

Phosphatidylcholine (PC) forms only lamellar mesophases in water, but it can be driven to self-assemble spontaneously into nonlamellar lyotropic liquid crystalline (LLC) mesophases by the addition of a third apolar component (oil) [2]. We report the

formation of a reverse micellar cubic mesophase of symmetry Fm3m (Q225) in ternary mixtures of soy bean PC, water, and an organic solvent, including cyclohexane, (R)-(+)-limonene, and isooctane, at room temperature [1]. The mesophase structure consists of a compact packing of remarkably large reverse micelles in a face-centered cubic (fcc) lattice, a type of micellar packing not yet reported for reverse micellar mesophases.
The mesophase spacegroup was identified by Small Angle X-Ray Scattering (SAXS) based on spacing ratios and peak intensities. The variations of structural parameters point out to a classical hard-sphere phase diagram, showing an order-disorder transition Fm3m-L_2 with an extended coexistence region. Form factor fitting in the pure L_2 phase and in the Fm3m-L_2 coexistence region yields quantitative estimations of the micellar low polydispersity (σ/R_c below 0.2), and PC interface rigidity $2k+\bar{k}$ of 1.6-2.0 k_BT.
The Fm3m structure is compared with the non-compact Fd3m structure found in the PC/water/α-tocopherol system. The compact Fm3m structure results mainly from (i) the release of lipid tail frustration and (ii) hard-sphere interactions between remarkably monodisperse micelles. The oil fills the geometric voids in the cell and modifies interface bending properties by penetrating the PC tails.
Acknowledgements: This study was funded by NESTEC Ltd.

[1] I. Martiel et al., *Langmuir* **29**(51), 15805-15812 (2013). [2] I. Martiel et al., *Adv. Colloid Interfac.* DOI:10.1016/j.cis.2014.03.005 (2014).

18-B Controlling Enzyme Activity and Kinetics by Physical Nano-Confinement

Wenjie Sun, J.J. Vallooran, A. Zabara and R. Mezzenga

Food and Soft Materials, D-HEST

Bicontinuous lipid cubic mesophases are widely investigated as hosting matrices for functional enzymes to build biosensors and bio-devices due to their unique structural characteristics. However, the enzymatic activitywithin standard mesophases (*in-meso)* is severely hindered by the relatively small diameter of the mesophase aqueous channels, which provide only limited space for enzymes, and restrict them into a highly confined environment. We show that the enzymatic activity of a model enzyme, Horseradish Peroxidase (HRP), can be accurately controlled by relaxing its confinement within the cubic phases'water channels, when the aqueous channel diameters are systematically swollen with varying amount of hydration-enhancing sugar ester.
The *in-meso* activity and kinetics of HRP is then systematically investigated by UV-vis spectroscopy, as a function of the size of aqueous mesophase channels. The enzymatic activity of HRP increases with the swelling of the water channels. In swollen mesophases with water channel diameter larger than HRP size, the enzymatic activity is more than double than that measured in standard mesophases, approaching again the enzymatic activity of free HRP in bulk water. We also showthat the physically-entrapped enzymes in the mesophases exhibit a restricted-diffusion-induced initial lag period and report the first observation of *in-meso* enzymatic kinetics significantly deviating from the normal Michaelis-Menten behavior observed in free solutions, with deviations vanishing when enzyme confinement is released by swelling the mesophase.

19-C Rheology of Hagfish Slime – a Marine Biopolymer

Lukas Böni, P.A. Rühs, E.J. Windhab, P. Fischer and S. Kuster

Food Process Engineering, D-HEST

Hagfish are able to gel immense quantities of water in seconds when provoked or stressed by predators through the release of exudate. This remarkable defense mechanism results in the formation of an elastic gel with high water content and fiber-like protein structures coated with mucins [1]. Whereas the chemical and physical composition of the hagfish slime are well known, little is known about the gelling and structuring potential of hagfish exudate. To address this shortcoming, both bulk and extensional rheology of hagfish slime in comparison with other marine based and gelling hydrocolloids was studied. By separating the different gel components, we were able to understand the rheological contributions and their synergistic effects. Additionally, through optimization of pH value, temperature, salt, and solvent conditions, the gel forming ability and thus the water entrapment were studied.

[1] D.S. Fudge et al., *J. Exp. Biol.* **208,** 4613-4625 (2005).

20-A Smart Dynamic Casting: A Robotic Fabrication of Complex Concrete Structures

Ena Lloret, R.J. Flatt, M. Kohler and F. Gramazio

Architecture and Digital Fabrication, D-BAUG

Concrete is a versatile material that can be obtained in almost any complex shape when placed into a formwork. However, to produce complex shapes a custom formwork is required. An energy consuming and waste intensive process given by the fact that all formwork is eventually discarded. In the inter-disciplinary research project Smart Dynamic Casting (SDC) the aim is to eliminate the need for custom

made formwork in the construction of complex concrete structures by exploiting the delicate period of time when this material transforms from soft to hard state.
The fabrication process described departs from conventional slipforming and combines it with robotics and concrete material science. Here, a formwork is attached to a 6-axis robotic arm, replacing the hydraulic jacks commonly used in slipforming. The formwork precisely shapes the concrete in the phase when it changes from soft to hard. The entire process is driven by the properties of the material that are continuously measured by a custom feedback system. This system automatically adjusts the slipping velocity additionally it informs when to mix and place the material. This enhanced robotic control combined with real time material feedback systems allows investigating the formability of concrete in a variety of geometries by expanding the movement of the formwork in time and space in a robotic slipforming process.

21-B Magnetic Excitations of J_1-J_2 Zigzag Chains in $SrDy_2O_4$ Frustrated Magnet

Nicolas Gauthier, A. Poole, M. Kenzelmann, A. Bianchi and J. Ollivier

Laboratory of Developments and Methods, D-PHYS, Paul Scherrer Institute

Due to competing interactions magnetically frustrated systems generally fail to reach a unique ground state but rather show macroscopic degeneracies and novel states of matter. Compounds of SrR_2O_4 family (R=Dy, Ho or Er) are geometrically frustrated rare-earth magnets and are good candidates to study strongly correlated fluctuating ground states [1]. Coexistence of two different magnetic orders, mostly short range, is observed in these compounds [2]. Considering these correlations and the strong single ion anisotropy, it has been established that these systems can be described by classical Ising zig-zag chains on two inequivalent sites [3]. We have studied the magnetic excitations in $SrDy_2O_4$ by inelastic neutron scattering with IN5 time-of-flight spectrometer at Institut Laue-Langevin. This compound does not have long range order down to 50 mK but only short range 1D correlations. The levels splitting due to the crystalline electric field is an essential aspect to understand this system. It explains the strong single-ion anisotropy and there is also evidence of dispersion of these levels due to magnetic interactions as observed in the inelastic spectra. The one-dimensional nature of this dispersion confirms the presence of 1D correlations and can be described from the Ising zig-zag chain model.

[1] H. Karunadasa et al. *Phys. Rev. B* **71**, 144414 (2005). [2] O. Young et al., *Phys. Rev. B* **88**, 024411 (2013). [3] A. Poole et al., arXiv:1401.3265 [cond-mat.str-el] (2014).

22-C Strain-Induced Metal-Insulator Transitions in d^1 Perovskites within DFT+DMFT

Krzysztof Dymkowski and C. Ederer

Materials Theory, D-MATL

We assess the effect of epitaxial strain on the electronic properties of the Mott insulator $LaTiO_3$ and correlated metal $SrVO_3$ using DFT + DMFT approach. We find that $LaTiO_3$ undergoes an insulator-to-metal transition under a compressive strain of about -2 %, consistent with recent experimental observations [1]. We show that this transition is driven mainly by strain-induced changes in the crystal-field splitting between the Ti t_{2g} orbitals. We demonstrate that a clear distinction between strain and interface effects is necessary for the understanding of emerging properties in oxide heterostructures.

[1] Wong et al., *Phys. Rev. B* **81**, 161101 (2010).

23-A Magnetic Properties of Multiferroic $TbMnO_3$

Natalya Fedorova, A. Scaramucci, C. Ederer and N.A. Spaldin

Materials Theory, D-MATL

We use ab initio calculations to investigate the magnetic properties of multiferroic $TbMnO_3$. At low temperatures $TbMnO_3$ demonstrates an incommensurate spiral ordering of Mn spins which is accompanied by appearance of spontaneous electric polarization driven by applied magnetic field. The establishment of such spin ordering is usually described within the framework of a Heisenberg model with competing nearest-neighbor and next-nearest-neighbor exchange interactions. However, our theoretical estimations of these interactions by ab initio calculations demonstrate a clear deviation from Heisenberg model.
We consider first the coupling between magnetic and orbital orderings as a main source of non-Heisenberg behavior in $TbMnO_3$, but conclude that it does not explain the observed deviation. We find that higher order exchange couplings should be taken into account for proper treatment of the magnetism in $TbMnO_3$.

24-B Superconductivity and Dipole Emergence in Lead Chalcogenides

Boris Sangiorgio, M. Fechner and N. Spaldin

Materials Theory, D-MATL

Lead telluride (PbTe) is a narrow gap semiconductor and a leading thermoelectric material at room temperature. At low temperature, thallium-doped PbTe exhibits a charge Kondo effect leading to superconductivity [1,2], and on heating an unusual structural symmetry lowering occurs, that has been associated with an emergence of local dipoles by Pb off-centering [3,4]. To identify the mechanisms behind these observations, we investigate the structural and electronic properties of (hole-doped) PbTe by means of density functional theory (DFT). We find that the choice of the exchange-correlation functional within DFT strongly influences the results, with PBEsol best able to reproduce most measured data. To understand the unusual low-temperature behavior, we perform a detailed characterization of the Fermi surface in collaboration with ongoing experimental studies. To address the occurrence of the reported local symmetry lowering we perform molecular dynamics calculations, which suggest large anharmonic effects in PbTe, but no static Pb off-centering.

[1] Y. Matsushita et al., *Phys. Rev. Lett.* **94**, 157002 (2005). [2] M. Dzero and J. Schmalian, *Phys. Rev. Lett.* 157003 (2005). [3] E.S. Bozin et al., *Science* **330**, 1660 (2010). [4] K.M.O. Jensen et al., *Phys. Rev. B* **86**, 085313 (2012).

25-A Clean and Efficient Transfer of Carbon Nanotubes for Device Fabrication

Valentin Döring, T. Süss and C. Hierold

Micro and Nanosystems, D-MAVT

In this study, a novel method for the transfer of carbon nanotubes (CNTs) from growth substrates to device substrates is introduced. Single-walled CNTs possess unique electronic and electromechanical properties making them promising building blocks for future sensor devices. In order to access these properties, integration into device structures is required. Chemical vapor deposition at high temperatures (typically 700-900°C) is commonly used for the synthesis of high quality single-walled CNTs. This step, however, puts constraints on the choice of materials if directly performed on the device substrate. On the one hand, the high temperature can adversely affect materials in the device structure. On the other hand, the synthesis process itself may be influenced or even inhibited by materials on the device substrate. Growing the CNTs on a growth substrate and then transferring them to the device substrate can circumvent these problems.
Different approaches for the transfer of CNTs using a sacrificial transfer medium exist. The novelty of the transfer process presented here is the use of a 900 nm thick lift-off resist (LOR, MicroChem) sacrificial layer. This layer is mechanically robust and easy to handle. But it can still be removed with mild chemistry, leaving only low amounts of residues on the transferred CNTs. The process requires only few, simple steps and inexpensive materials. Furthermore, CNT field effect transistors with clear transistor characteristics have successfully been fabricated with CNTs transferred using the novel method. This shows that the process is a robust, clean, and efficient alternative to existing CNT transfer processes based on other sacrificial transfer media.

26-B Pulsed Bi_2Te_3 Plating for Large-Scale Production of Thermoelectric Converters

Lukas Durrer, M. Kugler, E. Schwyter*, T. Helbling, W. Glatz* and C. Hierold

Micro and Nanosystems, D-MAVT

Heat-flux sensors convert thermal flux through the sensor element into a voltage by means of the Seebeck effect. The difference in electrical potential depends on the amount of heat passing through the sensor. This type of sensor can be used to investigate building isolations, in calorimetry equipment or for laser power applications and sun radiation measurements.
greenTEG in collaboration with ETH Zürich developed a large scale production process for thermoelectric converters. The process is based on electroplating Bi_2Te_3 into a structured polymer matrix and allows up-scaling of the device production. greenTEGs first product the gSKIN®, a highly sensitive and robust heat flux sensor, has been launched in the beginning of 2013.
Here, the development of the Bi_2Te_3 compounds is presented. Cyclic voltammetric, chronoamperometric and chronopotentiometric investigations resulted in a pulse plating method of high quality thermoelectric Bi_2Te_3 with control on stoichiometry. It will be shown that the sensitivity of the heat flux sensors strongly depends on the morphology and the thermoelectric properties of the plated material, which in turn can be tuned by the plating parameters.

* affiliation: greenTEG AG

27-C Optimizing the Performance of Substrate-Bound CNFETs by Utilizing an Alumina Protective Layer

Wei Liu, K. Chikkadi, M. Haluska and C. Hierold

Micro and Nanosystems, D-MAVT

Carbon nanotube field-effect transistors (CNFETs) exhibit superior diameter-normalized current density over silicon-based devices. However, it is critical to preserve the clean surfaces of single-walled carbon

nanotubes (SWNTs) acting as channels in CNFETs. Reviewing the lithography-based fabrication processes, resist residues existing on/around nanotubes largely degrade the CNFET performance. We present an approach to preserve the cleanliness of SWNTs by using an embedded protective layer. A thin layer of alumina is deposited on substrate by means of atomic layer deposition (ALD). This protective layer prevents direct contact of the nanotubes with the image resists during the device fabrication. The alumina is easily and completely removed from the future electrode contact area prior to metallization. No recognizable damages to SWNTs are caused by the alumina etchant. Based on the comparison of 491 devices, it is shown that the median values of on-resistance and hysteresis width are respectively reduced by 45% and 77% by using the alumina protective layer. The dispersions of on-resistance and hysteresis width are also significantly narrowed. The approach is extendable to nanotube-related large-scale fabrication processes. Owing to the alumina layer protecting CNTs, oxygen plasma ashing could be applied to further improve the cleanliness of CNTs. The impact of oxygen plasma treatment through the alumina layer on CNT properties monitored by Raman spectroscopy will be also presented.

28-B Nanocapacitors by Strain-Induced Defect-Polarization Coupling in $SrMnO_3$ Films

Carsten Becher, L. Maurel, M. Lilienblum, M. Trassin, D. Meier, C. Magen, E. Langenberg, L. Morellon, P.A. Algarabel, J. Blasco, J.A. Pardo, U. Aschauer, N. Spaldin and M. Fiebig

Multifunctional Ferroic Materials, D-MATL

Epitaxial strain can stabilize new matter phases in thin films and is thus a degree of freedom to increase functionality. Here, we use pulsed laser deposition to grow 20 nm thin $SrMnO_3$ films under tensile strain levels of about 2%. High resolution X-Ray diffraction and transmission electron microscopy were carried out to confirm the crystalline quality of the tetragonal films. Using optical second harmonic generation (SHG), we demonstrate the emergence of a polar state for these films confirming theoretical predictions. Furthermore, scanning probe microscopy reveals an intriguing conductance pattern in the polar phase that is assembled by electrically isolated regions. We propose strain-induced oxygen vacancy formation as origin for this spatial confinement of charges. Therefore, each of the regions can be charged and discharged individually, which makes them a novel type of strain-induced nanocapacitors.

29-A Flipping Ferroelectric Domains with Magnetic Fields

Naëmi Leo, D. Meier, J. White, M. Kenzelmann and M. Fiebig

Multifunctional Ferroic Materials, D-MATL

Strong correlations between spin and charge degrees of freedom already play a major role in today's digital data storage technology. A major goal in modern material research is to improve such interactions, as well as to find new materials that can be used to a technological advantage.
Multiferroic materials with coexisting ferromagnetic and ferroelectric orders exhibit such unusual cross-couplings. A particular interesting member of this material class is olivine Mn_2GeO_4, where complex spin order induces a spontaneous polarization whose sign can be completely flipped by a small magnetic field. However, it is unclear how the ferroelectric domains act upon this reversal, as spatial resolved measurements are challenging.
Here, optical second harmonic generation (SHG) allows to probe and image magnetic and electric domains in Mn_2GeO_4 and investigate their reaction to applied fields: Switching the ferroelectric polarization by an applied electric field involves nucleation and growth of domains with opposite polarity, whereas – surprisingly – the domain structure remains robust under the magnetic-field-induced polarization reversal.
Understanding the microscopic interactions leading to this remarkable and efficient cross-coupling might give insight to material properties promoting such unusual behaviour and might give hints to the purposeful design of multiferroic materials optimized for technical applications.

30-B Exotic Ferroelectric Order in Multiferroic h-$YMnO_3$

Martin Lilienblum, S. Manz, S.M. Selbach, S.M. Griffin, N.A. Spaldin and M. Fiebig

Multifunctional Ferroic Materials, D-MATL

Universal scaling laws, interfacial nano-electronics, and topological textures are currently studied using hexagonal rare earth manganites ($RMnO_3$, R= Sc, Y, Dy-Lu) as model system. In spite of the remarkably broad interest in the system, surprisingly little is known about fundamental material properties such as the emergence of the ferroelectric polarization and the associated domain formation. Here we solve the controversy about the emergence of the spontaneous polarization and its coupling to the underlying structural distortion by applying a combination of characterization methods, including scanning probe microscopy (SPM) and nonlinear optics.

Via thermal treatments closely to the structural transition and subsequent SPM investigations we find that the exceptionally robust ferroelectric domain structure is predetermined by the primary distortive order without influence of the improper polarization.
We used optical second harmonic generation from 100 K to 1450 K in order to probe the polarization directly and contact-free, since dielectric measurements are not suitable due to high electrical conductivity of the compound. We find that only a single phase transition exists in which the polarization emerge along with the structural distortion yet with an unexpectedly pronounced delay. Thus the polarization reaches only 10% of its saturation value at a temperature at which the distortion strength exceeds already 60%. A phenomenological analysis of the unique temperature dependence allows us to quantify the coupling between polarization and structural distortion.

31-C Tuning the Electronic Transport Behavior at Functional Ferroelectric Domain Walls

Jakob Schaab, M. Lilienblum, M. Fiebig and D. Meier

Multifunctional Ferroic Materials, D-MATL

Domain walls in ferroelectric complex oxides gain great attention in modern materials research, because they represent structurally perfect interfaces with unusual physical properties. These domain walls can for instance be electrically conducting even when the surrounding bulk material is an insulator so that they may serve as wires with atomic-scale dimensions in nano-electronics devices. At present, however, the current densities measured at ferroelectric domain walls are still rather small and identification of possible roadmaps for engineering their electronic behavior is highly desirable.
Here, we present an approach for modifying the domain wall conductance by chemically doping a ferroelectric semiconductor with either p-type or n-type charge carriers. Within our p-type model system, i.e. hexagonal $ErMnO_3$, positively and negatively charged ferroelectric domain walls are formed at which mobile holes deplete and accumulate giving rise to suppressed and enhanced conduction properties, respectively. By doping 1% Ca into the system and hence increasing the number of p-type carriers we managed to tune the domain wall conductance by a factor of about 10^3 and further reduced the electronic domain wall width by about 30%. The results demonstrate that chemical bulk doping is a promising and efficient route for controlling the electronic domain wall performance offering new perspectives for domain wall engineering in semiconducting ferroelectrics.

32-A Nanoparticle-Based Multicomponent Aerogel Monoliths

Florian Heiligtag, F. Rechberger, M.J.I. Airaghi Leccardi and M. Niederberger

Multifunctional Materials, D-MATL

Nanoparticle (NP) based aerogels represent a sophisticated class of materials with low density, high surface area, open porosity, and excellent noise and heat insulating capabilities. A synthesis route via the self-assembly of preformed NPs offers beneficial effects in comparison to traditional sol-gel approaches. Defined crystallinity and composition of the NP building blocks and a defined mixture of different building blocks enables the preparation of complex aerogel structures that are not accessible by molecular sol-gel processes. This results in improved properties and functionalities. In particular, examples in the area of photocatalysis [1] and luminescence [2] have been reported.
In this work we present titania NPs as building blocks for photocatalytically active aerogels. These titania structures show good specific surface area, high porosity and well defined crystallinity. By a careful control of the gelation process of well dispersed nanoparticle building blocks, anatase aerogels are produced with outstanding translucency.
These anatase aerogel structures serve as matrix for the incorporation of several other types of nanoparticles and nanowires, offering unique possibilities for the improvement of the photocatalytic properties and for the implementation of further functionalities. Exemplarily the improvement of the photocatalytic properties can be shown by the incorporation of gold NPs [1]. An excellent example for the implementation of further functionalities is the addition of magnetic Fe_3O_4 NPs. This adds magnetic properties to the photocatalyst and enables the controlled release of the catalyst to a reaction solution and the controlled removal therefrom.
The use of preformed building blocks and the easiness to control the gelation process allows the production of aerogels with locally well-defined content of different nanoparticles of specific shape and crystallinity, resulting in the production of complex layered aerogel structures.

[1] F.J. Heiligtag et al., *J. Mater. Chem.* **21**, 16839 (2011). [2] J.L. Mohanan et al., *Science*, **307**, 397 (2005).

33-B In-Situ X-Ray Absorption and Emission Spectroscopy Study of the Interaction between CO_2 and Lanthanum-Oxycarbonate Nanoparticles

Ofer Hirsch

Multifunctional Materials, D-MATL

Recently, sensitivity of rare-earth-oxycarbonates based sensors to CO_2 was reported. However, the physical origin of the charge transfer between a relatively inert CO_2 and rare-earth-oxycarbonates, which leads to increase of the sensor's resistance is not understood. Here, the challenge is to collect the complementary information about the reversible changes of the La state at the surface of nanoparticles and the orbitals that are involved in bonding during the CO_2 interaction. We overcome this task by increasing the surface area of $La_2O_2CO_3$ nanoparticles and increasing the porosity of the sensing layers. This morphology is chosen to increase the number of sites available for the interaction with CO_2 at the surface of nanoparticles that enables the application of in-situ HERFD X-ray absorption and emission spectroscopy to study the origin of this interaction. We fabricate, the sensitive layer in two steps: First, we synthesize $La(OH)_3$ nanoparticles in organic solvent using a microwave oven, with average size of 8 nm. Second, we dip-coat those nanoparticles on a substrate and anneal them under air to obtain a porous film of $La_2O_2CO_3$ particles with average particle sizes of 11 nm and a thickness of 2 mm. Such a sensor shows sensitivity to CO_2 with a sensor signal of more than 15 in synthetic air with 50% relative humidity at 250 °C and 10 000 ppm of CO_2. Measuring the lanthanum L_3 edge of this sensor under those conditions reveals a rise in the intensity during CO_2 exposure and a sharpening of the white line, which represents oxidation of the La-atoms. While XAS gives information about the unoccupied states, valence-to-core XES contains information about the occupied valence states just below the Fermi-energy. The two main features are at 38.5 eV and 10.1 eV below the elastic peak. Interestingly, even the deeper states change during the interaction with CO_2.

34-C Puzzling Mechanism Behind a Simple Synthesis of Cobalt and Cobalt Oxide Nanoparticles: In Situ Synchrotron X-Ray Absorption and Diffraction Studies

Malwina Staniuk, O. Hirsch, N. Kränzlin, R. Böhlen, W. van Beek, P.M. Abdala and D. Koziej

Multifunctional Materials, D-MATL

Here, we show a simple approach to synthesize cobalt and cobalt oxide nanoparticles in an organic solvent. We find that the cubic Co_3O_4 nanoparticles can be easily obtained, even at temperatures as low as 80 °C. Moreover, exactly the same reaction at 180 °C leads to metallic Co nanoparticles. Thus, in addition to the synthetic efforts, we study the mechanism of occurrence of oxidation and reduction of a Co^{2+} precursor in benzyl alcohol. Remarkably, the in situ X-ray absorption and diffraction measurements of the synthesis at 140 °C reveal that oxidation of Co^{2+} to $Co^{3+/2+}$ and reduction of Co^{2+} to Co^0 reactions take place simultaneously. It is followed by a rapid formation of Co_3O_4 nanoparticles and its consecutive solid-state reduction to CoO. In parallel, metallic Co nanoparticles begin to grow. In addition, Multicomponent Curve Resolution–Alternating Least Squares (MCR-ALS) analysis of X-ray absorption spectroscopy (XAS) data efficiently reveals the nontrivial inter-dependence between four different reactions. Our strategy to control reduction and oxidation of Co-based nanoparticles as they grow opens up an elegant pathway for the one-pot-synthesis of the hybrid materials for energy-related applications.

35-B Charge Transport Kinetics in PbS Nanocrystal-Based Solar Cells

Nuri Yazdani, D. Bozyigit, O. Yarema, M. Yarema and V. Wood

Nanoelectronics, D-ITET

Significant progress in the optimization of lead sulfide (PbS) colloidal nanocrystal solar cells has been made in recent years and power conversion efficiencies of 8.6% have been reached. For different device architectures (i.e. metal-semiconductor-metal and heterojunction), different ligands and PbS film thicknesses have yielded the best solar cell performances to date. While built in fields extended through the QD films driving drift currents are expected to play a role in charge transport, recent work demonstrated that equivalent photovoltages can be achieved across metal/PbS and metaloxide/PbS junctions in the absence of a built in electric field as a result of asymmetry in the transfer kinetics of the charge carriers into the contacts. The influence of the choice of ligands and contacts on the charge transport remains unclear.

We present time of flight measurements on PbS nanocrystal-based solar cells using various nano-crystal sizes. Characterization of the short circuit transients at various bias voltages enables the determination of hole mobility in the nano-crystal solid films. A discussion of the nanocrystal size dependence of the hole mobility is presented, along with comparison to existing theory.

36-A Influence of the Film Thickness on Fragmentation, Adhesive Failure and Contact Damage of Diamond-Like Carbon (DLC) Coated Titanium Substrates

Daniel Bernoulli, A. Wyss, K. Häfliger, K. Thorwarth, G. Thorwarth, R. Hauert and R. Spolenak

Nanometallurgy, D-MATL

Diamond-like carbon (DLC) coated friction pairs are well-known for their long durability and outstanding tribological behavior. However, wear and loose particles trapped between the friction pairs can lead to the appearance of high pressure on the DLC coating and may result in contact damage, fragmentation and adhesive failure. The influence of the DLC film thickness on these three effects is presented in this talk. The contact damage upon indentation was analyzed by finite element analysis and experimental work. For thicker films circumferential and horizontal cracks are present in the DLC while for thin DLC films pronounced plastic deformation of the substrate occurs. The fragmentation analysis reveals that a very high DLC fracture strength can be achieved by keeping the DLC film thickness <1 μm. Adhesive failure is absent for very thin DLC films, however, for thicker films the total delaminated area depends strongly on the DLC film thickness. For all three cases an optimal DLC film thickness is presented.

37-B Polymer and Polymer Nanocomposite Patterning by Dip Pen Nanolithography

Ayse Cagil Kandemir, D. Erdem, M. Niederberger and R. Spolenak

Nanometallurgy, D-MATL

Dip Pen nanolithography (DPN), is a tip based nanolithography method, which serves a novel approach to produce nano and micro-scaled patterns owing to its high resolution and pattern flexibility. Being a constructive lithography method, DPN delivers materials by using the tip of a cantilever as pen and substrate as paper. It is confirmed that variety of materials could be patterned via DPN on different surfaces. In literature, DPN studies on polymer nanocomposites mostly focuses on use of polymer matrix as delivery medium for nanoparticle deposition and subsequent removal of the loosely-bounded matrix material by heating or oxygen plasma after deposition.

There are two objectives of this study; first writing polymer patterns to investigate capabilities of DPN and second constructing polymer nanocomposite patterns to have synergistic properties of both matrix and additive materials.

As additive material, cobalt iron oxide ($CoFe_2O_4$) particles with 5-7 nm particle size range are used [1]; which is subsequently embedded in polymer matrix to produce nanocomposite inks. A contact mode AFM tip is utilized in order to write dot and line patterns with varying dwell times on silicon substrate. Characterization was conducted by SEM and AFM. SEM images confirmed that particles are deposited with polymer. It is observed that ink viscosity affects ink delivery as there is an inverse relation between ink viscosity and depletion time. This study also yielded the optimal conditions to produce consistent nanocomposite patterns with DPN. The studied writing conditions, such as particle concentration, ink composition, humidity range etc. yielded compatible dot sizes with writing speeds.

[1] I. Bilecka et al., *J. Sol-Gel Sci. Technol.* **57**(3), 313–322 (2010).

38-C Ion Beam Induced Selective Grain Growth and Texturing in Tungsten Thin Films

Huan Ma, C.M. Muller, A.S. Sologubenko, M. Seita and R. Spolenak

Nanometallurgy, D-MATL

Ion beam irradiation along channeling direction will lead to selective grain growth in crystalline materials. In contrast to normal grain growth by heat treatment, where the movement of grain boundary is driven by grain boundary curvature, the driving force for ion beam induced selective grain growth mainly come from the difference of volume free energy between grains oriented for channeling and those randomly oriented. With less irradiation damage, grains oriented for channeling are selected to grow at the expense of the others and, consequently, leading to texturing. In this study, we investigated the selective grain growth and texturing behavior in (110) fiber textured W thin films upon 4.5 MeV Au ion irradiation. Two channeling systems (<111> and <100>) were activated simultaneously during irradiation due to their small angular spacing and the relatively large orientation distribution of the as deposited film. In addition, selective grain growth was found to be very sensitive to irradiation temperature. Irradiation at liquid nitrogen temperature lead to continuous growth of selected grains as function of ion fluence while irradiation at room temperature only slightly increased the grain size at low fluence and had no further obvious effect. This was attributed to the temperature dependence of defect annealing processes during irradiation. The amount of surviving defects upon low temperature irradiation was expected to be higher than that upon room temperature irradiation and, therefore, the driving force in the former case was higher than the latter.

39-A Mechanical Properties of Broad-Band Bragg Reflector Coatings for Dental Implants

Daniel Muff and R. Spolenak

Nanometallurgy, D-MATL

Due to their inherent dark grey color, titanium dental implant screws can cause undesired darkening of the peri-implant mucosa. Ceramic multilayer thin film structures, so called Bragg reflector coatings, have been developed to increase their reflectance.
Besides the esthetic function, the mechanical integrity of the coatings is crucial. As implants bend during chewing motions, coatings have to withstand compressive and, more critically, tensile strains. Therefore, in-situ tensile testing of the ceramic films on polyimide and titanium substrates has been carried out in optical and scanning electron microscopes in order to determine their fracture and delamination behavior.
It was found that the strain at onset of fragmentation decreases with increasing film thickness or number of layers. Cracking and delamination of a broad-band Bragg reflector coating on titanium occurs at strains higher than the elastic limit of the substrate. By tuning the interface chemistry, further improvements in cracking and delamination behavior can be achieved.

40-B Optical Properties and Durability of Dental Coatings

Christina Pecnik and R. Spolenak

Nanometallurgy, D-MATL

Implant restorations have to fulfill certain requirements in terms of mechanical, biocompatible and esthetic properties. Titanium (Ti) and its alloys meet these demands since these materials have excellent physical and chemical properties. However, in certain cases a gray discoloration of the soft tissue can be observed using Ti implants, resulting in an undesired esthetic outcome. Therefore, a new coating system which combines the mechanical properties of metals with the good optical properties of ceramics would enhance the esthetics of dental implants. Above all, clinical success of dental implant systems depends strongly on their reliability. The coating should not only be esthetically pleasing and chemically durable, but it should also withstand cyclic stresses as they are present during chewing motions.
In this study, four different coatings (Ti-ZrO_2, Ti-Al-ZrO_2, Ti-Ag-ZrO_2 and Ti-Bragg (TiO_2/SiO_2)) were deposited on Ti substrates by reactive magnetron sputtering. The coating structure and thickness were different for each coating system and their color is formed by mirror and light interference phenomena. The purpose of these coating systems is to increase the brightness of the underlying substrate material and therefore to avoid esthetic complications of dental implants. *In vitro* color evaluation showed that the optical appearance of soft tissue was improved by coatings developed in this study. The mechanical properties of these coating systems were achieved by nanoindentation. Examinations with the scanning electron microscope revealed various cracking scenarios. The fracture toughness (K_c) could be easily determined for the coating system Ti-Bragg, since this system behaves brittle and showed exemplary crack patterns to quantify K_c properly. By contrast, the systems Ti-ZrO_2, Ti-Al-ZrO_2 and Ti-Ag-ZrO_2 showed less cracking at indent corners, especially coating systems with Al or Ag, which exhibited a high resistance to crack propagation due to their ductile intermediate layer.

41-C Finite Element Approach for Gas Flow Modelling in the Early Arcing Stage

André Röthlisberger and R. Spolenak

Nanometallurgy, D-MATL

Arc erosion of the contact materials during switching operations in SF_6 gas-isolated high voltage circuit breakers limits the lifetime of these devices due to material degradation. Understanding the process of arc erosion, and consequently the factors involved in material degradation of the WCu arcing contacts, is a prerequisite for the design of new arcing contact assemblies. It is therefore important to understand the evolution of the temperature profile in the arcing contacts during and after switching operations of the circuit breaker, since erosion is mainly due to melting and evaporating of the contact materials. For this purpose preliminary studies for gas flow and arc extinction have to be conducted. Setting up in-situ experiments at the high voltage level is very demanding and expensive. Multiphysics finite element modelling can yield access to this desired information by means of solving the magneto-hydrodynamic (MHD) equations in the gas phase, yielding the transport properties for heat flux and therefore enabling the calculation of the temperature profile in the cathode. In this work a preliminary study for gas flow solving the compressible turbulent Reynolds-averaged Navier-Stokes (RANS) equations in a simplified breaker assembly is conducted. The presented results will serve as a basis for further more complex modelling approaches for the temperature profile evolution in the cathode and shall highlight the possibility of FE modelling to help design possible new arcing contacts assemblies.

42-A Size-Dependent Plasticity in Ionic Crystal Sytems: The Influence of Temperature, Orientation and Doping Level

Yu Zou and R. Spolenak

Nanometallurgy, D-MATL

Size dependence of plasticity is generally observed and intensively studied in metallic systems but is rarely investigated in ionic crystal systems. In this study, the microcompression technique is applied to study the size effect on plasticity in four typical ionic crystals with rocksalt structure, i.e. NaCl, KCl, LiF and MgO. How the test temperature, orientation and doping level influence size-effect exponents is investigated and compared. In contrast to NaCl and KCl, a strong temperature and orientation dependence on size effect for LiF and MgO was observed. For example, [100] and [111]-oriented LiF have size-effect exponents of -0.7 and -0.4, respectively, but both [100] and [111]-oriented KCl have the same exponent of -0.7. In addition, the doping in NaCl only changes the absolute strength value but does not change the size-effect exponent. The influence of temperature, orientation and doping level on size effect could be attributed to the residual Peierls stress at test temperatures.

43-C Air Entrainment Simulation of Tube-Enclosed Flame Aerosol Synthesis of Nanoparticles by Computational Fluid Dynamics

Oliver Brenner and O. Waser

Particle Technology Laboratory, D-MAVT

Synthesis of functional nanoparticles requires more and more refined production processes. Enclosing the scalable flame spray pyrolysis (FSP) process facilitates synthesis of a number of sophisticated nanomaterials [1].
Enclosing the classic FSP reactor by such a tube-enclosure typically leads to larger primary particles since the natural air entrainment (AE) is blocked leading to longer particle residence time at high temperature and higher precursor concentrations – both enhancing coagulation and subsequent primary particle growth. Furthermore, recirculation of high temperature aerosol within the tube enclosure could extend the residence time leading to even larger particles and unfortunately broad particle size distribution [2].
Here commercial software (Ansys Fluent) and existing code [3] were used to solve flow and energy equations but also droplet dynamics and global chemical reactions in order to visualize above processes and propose improvements to the current geometry. The influence of AE flow rate on vortex formation, temperature distribution and resulting residence time distributions (RTD) will be studied for various tube lengths and compared to experiments where possible.
Preliminary results show that low AE induces big recirculation vortices inside the enclosing tube (in agreement with literature) where high AE tends to displace the combustion products towards the tube center without vortices. Tube exit temperatures for high AE show very good agreement with experiments while at low AE still significant deviation is present due to radiation heat loss.

[1] R. Strobel and S.E. Pratsinis, *J. Mater. Chem.*, **17**, 4743-4756 (2007). [2] O. Waser et al., *J. Power Sources,* **241**, 415-422 (2013). [3] A.J. Grohn et al., *Chem. Eng. J.*, **191**, 491-502 (2012).

44-B Effect of Ba and K in Rh/Al_2O_3 Catalysts for CO_2 Hydrogenation

Robert Büchel, A. Baiker and S.E. Pratsinis

Particle Technology Laboratory, D-MAVT

The effect of Ba and K addition to Rh/Al_2O_3 catalysts for CO_2 hydrogenation was investigated. Catalysts with preferential deposition of 1 wt% Rh either on the alumina support or the Ba or K component was prepared by the two nozzle flame spray pyrolysis method. The pure Rh/Al_2O_3 catalyst as well as the Ba-containing catalysts showed a high selectivity to CH_4 below 500 °C with a maximum yield at 400 °C. Above 400 °C, the reverse water gas shift reaction leading to CO and H_2O started to become dominant, in accordance with thermodynamics. In contrast, the K-containing catalysts produced no CH_4, all CO_2 was directly converted to CO in the entire temperature range (300-800 °C). Preferential deposition of the Rh on the additive components (Ba, K) or the alumina support had comparably little effect on the catalytic behavior.

45-C Coagulation of Fractal-Like Aerosols in the Transition Regime

Eirini Goudeli, M.L. Eggersdorfer and S.E. Pratsinis

Particle Technology Laboratory, D-MAVT

Gas-phase processes offer a proven scalable route for the synthesis of nanoparticles for the large scale production of commodities like fumed silica, carbon black and pigmentary titania [1]. Such processes allow the production of particles with different structures (e.g. spheres, rods, aggregates and agglomerates). Modeling the particle growth is of utmost importance for the design of aerosol reactors. There particle dynamics span 10 and 15 orders of magnitude in length and time, respectively, and determine particle structure effects influencing the electrical conductivity and mechanical stability of product films and powders. Agglomeration (i.e.

particle formation with loosely attached primary particles) occurs both in environmental and industrial processes, especially in low temperature regions where sintering or coalescence are rather slow. The dominant coagulation mechanism is cluster-cluster agglomeration leading mainly to the formation of filamentary structures that are attractive in nanocomposites and particle suspensions (paints or polishing slurries).
Here the growth and detailed structure of fractal-like particles undergoing Brownian coagulation is investigated in the entire particle size range, from the free molecular to the continuum region. Particles in the free molecular limit follow random ballistic trajectories described by an event driven method whereas in the near continuum and continuum regime Langevin Dynamics effectively describe their diffusive motion (random walk). The method is applied for aerosol coalescence and coagulation-agglomeration (e.g. without any coalescence). The evolution of the properties of the resulting fractal-like agglomerates (i.e. geometric standard deviation and structure) is traced in the transition regime and their self-preserving values and size distributions are validated at the known limits of the free molecular and continuum limit at dilute conditions.

[1] S.E. Pratsinis, *AIChE J.* **56**, 3028-3035 (2010).

46-A Scale-Up of Nanoparticle Synthesis by Flame Spray Pyrolysis: The High Temperature Particle Residence Time

Arto Gröhn, S.E. Pratsinis and K. Wegner

Particle Technology Laboratory, D-MAVT

The scaling-up of nanoparticle synthesis by a versatile flame aerosol technology (flame spray pyrolysis, FSP) is investigated numerically and experimentally for production of ZrO_2. A three-dimensional computational fluid dynamics model is developed accounting for combustion and particle dynamics by an Eulerian continuum approach coupled with Lagrangian description of multi-component spray droplet atomization, transport and evaporation. The model allows extracting the high-temperature particle residence time (HTPRT) that is governed by the dispersion gas to precursor liquid mass flow ratio as well as the flame enthalpy content. The HTPRT is shown to control the primary particle and agglomerate size, morphology and even ZrO_2 crystallinity in agreement with experimental data. By keeping the HTPRT constant the production rate for ZrO_2 nanoparticles could be scaled up from ~100 to 500 g/h without significantly affecting product particle properties, revealing the HTPRT as a key design parameter for flame aerosol processes.

47-B Visible-Light Active Black TiO_2-Ag/TiO_x Particles

Fujiwara Kakeru, Y. Deligiannakis, C.G. Skoutelis and S.E. Pratsinis

Particle Technology Laboratory, D-MAVT

Visible-light active materials are sought in photocatalysis and solar energy utilization. Here a material architecture active under visible-light and comprising of titanium suboxide (e.g. Ti_4O_7, Ti_3O_5) layers onto nanosilver on nanostructured TiO_2 is formed by flame aerosol technology. Abundant combustion intermediates present during flame synthesis of these materials partially reduce TiO_2 and induce strong metal-support interactions (SMSI) resulting in crystalline Ti-suboxides as determined by X-ray diffraction. The growth of such suboxides can be controlled through their flame spray synthesis conditions allowing for tuning the light absorption intensity in the visible spectrum. The as-prepared Ti-suboxides are stable upon annealing in air, at least, up to 350°C for two hours. Their presence on the Ag/TiO_2 particle surface and efficiency in generating photoinduced charge separation under visible light is demonstrated by electron paramagnetic resonance spectroscopy. Under visible light ($\lambda > 400$ nm), these nanoparticles exhibit strongphoto-reduction of cationic species (Cr^{6+}) and photo-oxidation of organics (methylene blue).

48-C Oxidative Coupling of Methane on Flame-Made Mn-Na_2WO_4/SiO_2: Influence of Catalyst Composition and Reaction Conditions

Rajesh Koirala, R. Büchel, A. Baiker and S.E. Pratsinis

Particle Technology Laboratory, D-MAVT

Mn-Na_2WO_4/SiO_2 catalysts containing 0 - 5 wt% Mn and 0 - 6 wt% Na_2WO_4 were prepared by flame spray pyrolysis (FSP) and tested for the oxidative coupling of methane (OCM) in a continuous flow microreactor at different reaction conditions (temperature, CH_4/O_2 feed ratio, space time). All catalysts were characterized by nitrogen adsorption, XRD, TEM and TPR. As-prepared catalysts were amorphous but SiO_2 gradually transformed to crystalline cristobalite during exposure to reaction conditions at 810 °C resulting in a strong reduction of the specific surface area (SSA). Both, cristobalite formation as well as SSA reduction had only a marginal influence on catalyst performance. Conversion and selectivity to C_2 compounds increased with Mn content up to 1.9 wt% and remained virtually constant up to 5 wt%, affording a constant C_2-yield of 17%. Increasing the Na_2WO_4 content was most effective up to 1 wt%, while at contents higher than 3 wt% the conversion declined. The 1.9%Mn-3%Na_2WO_4/SiO_2 catalyst exhibited

the highest C_2-yield of 18.5% at a selectivity of 68.6%. The flame-made catalyst and a corresponding wet-impregnated reference catalyst showed stable conversion when exposed to longer time-on-stream but the C_2-yield of the former was significantly higher due to both higher selectivity and conversion.

49-A Photothermal Killing of Cancer Cells by the Controlled Plasmonic Coupling of Silica-Coated Au/Fe_2O_3 Nanoaggregates

Fabian Starsich, G.A. Sotiriou and S.E. Pratsinis

Particle Technology Laboratory, D-MAVT

Tumor ablation by thermal energy via the irradiation of plasmonic nano-particles is a relatively new oncology treatment [1]. Hybrid plasmonic-superparamagnetic nanoaggregates (50–100 nm in diameter) [2] consisting of SiO_2-coated Fe_2O_3 and Au (≈30 nm) nanoparticles were fabricated using scalable flame aerosol technology [3]. By finely tuning the Au interparticle distance using the SiO_2 film thickness (or content) the plasmonic coupling of Au nanoparticles can be finely controlled bringing their optical absorption to the near-IR [4] that is most important for human tissue transmittance [5]. The SiO_2 shell facilitates also dispersion and prevents the reshaping or coalescence of Au particles during laser irradiation, thereby allowing their use in multiple treatments. Their effectiveness as photo-thermal agents is demonstrated by killing human breast cancer cells with a short, four minute near-IR laser irradiation (785 nm) at low flux (4.9 W cm^{-2}).

[1] G.A. Sotiriou et al., *Adv. Funct. Mater.* DOI: 10.1002/adfm.201303416 (2014). [2] G.A. Sotiriou et al., *Chem. Mater.* **23**(7), 1985-1992 (2011). [3] S.E. Pratsinis, *AIChE J.* **56**(12), 3028-3035 (2010). [4] U. Kreibig and L. Genzel, *Surf Sci.* **156**, 678-700 (1985). [5] R. Weissleder, *Nat. Biotechnol.* **19**(4), 316-317 (2001).

50-C High Performance Fiber Reinforced Light-weight Concrete

Paula Bran Anleu, P. Suraneni and R.J. Flatt

Physical Chemistry of Building Materials, D-BAUG

This study presents basic information on mechanical properties of fiber-reinforced lightweight concrete (FRLC). Concrete's strength decreases significantly with decreasing density and therefore, there exist few examples of structural grade concretes with densities below 1600 kg/m^3. Here we show the development of relatively high performance light-weight concrete in the 1300 – 1600 kg/m^3 density range. Different fibers at different volume fractions were investigated, and a thorough comparison is shown. Compressive strength tests were performed to determine basic properties of FRLC. Compressive strengths of up to 36 MPa were obtained at 28 days. In general, bending strength values were low, but the use of more than one fiber type improved the bending strengths to up to 8 MPa at 28 days. The major factors controlling compressive and bending strengths in these lightweight concrete mixes are also discussed.

51-B Predicting the Future of Salt-Weathered Stone

Francesco Caruso, A.M. Aguilar Sanchez, G.W. Scherer and R.J. Flatt

Physical Chemistry of Building Materials, D-BAUG

Soluble salts are among the main causes responsible for the weathering of stone. This is a major issue in different fields: conservation science, geotechnics, geomorphology, and concrete science. For such a reason and to establish the durability of a stone against salt crystallization, a wetting-drying test with sodium sulfate solutions has been used since the 19th century. Despite its wide use, the quantitative connection to the mechanical damage of stone has been so far missing.
In this work, we validated a simple – yet powerful – approach to give a poromechanical interpretation of the sodium sulfate test and predict the onset of damage in salt-weathered stone.

52-C Impact of Polycarboxylate Superplasticizer on Polyphased Clinker Hydration

Delphine Marchon, P. Juilland, M. Jachiet and R.J. Flatt

Physical Chemistry of Building Materials, D-BAUG

The balance between the silicate, aluminate and sulfate phases in cement is one of the most important aspects during hydration. It is well known that when the supply of sulfates is too low to prevent fast aluminates hydration, silicates hydration is retarded. Comb-shaped polycarboxylates ether (PCE) superplasticizers are also known for impacting cement reactions, leading to strong hydration retardation.
In this study, the hydration of a synthetized polyphased clinker with 80%wt. alite and 20%wt. C_3A with hemi-hydrate has been studied in presence of a PCE added either directly in the water or later in the paste.
Calorimetric and XRD measurements have shown that the effect of the PCEs on the hydration of this model binder varies strongly with the time of addition of the polymer. When the PCE is added with a small delay, hydration is retarded with a

slight imbalance of sulfate and aluminate phases, as can be observed in OPC hydration. However, when PCEs are added directly in the mixing water, the aluminate peak is drastically accelerated and the silicate one delayed, showing a clear transition from a balanced system to a less sulfated one. The reasons for this transition are discussed with respect to the type and availability of sulfate sources and the precipitation of ettringite, clearly influenced by the polymer.

53-A Filling in the Gaps of Alite Hydration

Prannoy Suraneni and R.J. Flatt

Physical Chemistry of Building Materials, D-BAUG

Cement is one of the most used materials in the world; however aspects of its early strength gain are still debated. We present here a new approach to study the early hydration reaction of cement, focusing in particular on the hydration reaction of alite (which is the main volumetric phase of cement and is most responsible for early strength development). Alite grains are embedded in epoxy, ground and polished, gold coated, and subsequently, micron-sized gaps are milled into the grains using a Focused Ion Beam. The samples are then immersed either in water or in solutions with varying concentrations of calcium hydroxide. The hydration reaction is stopped at desired ages using solvent exchange and the gaps are imaged using a Scanning Electron Microscope. This method offers several advantages over conventional methods to monitor the alite hydration process. In particular, we can study dissolution kinetics and hydrate growth morphology in a reproducible manner using a setup that mimics particles in close contact. The effects of solution used and admixtures on the dissolution kinetics and growth morphology are discussed. The limitations of the method are acknowledged and complimentary experimental methods are noted. Results are shown with other materials as well, and we demonstrate that this is a method that can be used to study general reactivity of a solid surface in contact with a solution.

54-C Clay Swelling in Anhydritic Claystones

Timothy Wangler, A. Shahab and R.J. Flatt

Physical Chemistry of Building Materials, D-BAUG

Anhydritic claystones, rocks with relatively high proportions of anhydrite and clays, are susceptible to expansion from exposure to water due to the anhydrite-to-gypsum transformation and the swelling of the clay fraction. One finds this rock in the troublesome Gipskeuper, and tunnels through this formation in Switzerland and southwestern Germany have experienced repeated floor heave events over many years, leading to expensive repairs [1]. Despite numerous studies that have spanned the past few decades [2–4], the relative contributions of the crystallization pressure due to the anhydrite-to-gypsum transformation and the swelling pressure of the swelling clays are still unknown due to the highly coupled nature of the problem.

Above a temperature of approximately 40°C, anhydrite becomes more stable than gypsum in the presence of water [5], and the anhydrite-to-gypsum transformation is effectively shut off. This has been demonstrated on actual samples of anhydritic claystone taken from the Chienberg Tunnel in Switzerland. By performing swelling experiments above this temperature, we are able to effectively decouple the two swelling phenomena and study clay swelling in isolation, enabling us to better quantify the contribution of clay swelling to this problem.

[1] G. Anagnostou et al., *Geomech. Tunn.* **3**, 567–572 (2010). [2] R. Nüesch and W. Baumann, *Geol. Rundsch.* **78**, 443–457 (1989). [3] R. Nuesch et al., 8th ISRM Congr. (1995). [4] E. Pimentel and G. Anagnostou, *Rock Mech. Rock Eng.* **46**, 1271–1285 (2013). [5] A.E. Charola et al., *Environ. Geol.* **52**, 339–352 (2007).

55-A Towards Germanium X-Ray Detector Monolithically Integrated on Silicon CMOS

Thomas Kreiliger, C.V. Falub, A.G. Taboada, F. Isa, S. Cecchi, G. Isella, R. Erni, P. Groening, P. Niedermann, R. Kaufmann, A. Dommann, L. Miglio, B. Batlogg and H. von Känel

Physics of New Materials, D-PHYS

Spatial resolution, sensitivity and costs of X-ray imaging detectors would greatly benefit from monolithic integration of an efficient absorber onto Si-CMOS readout circuits. However, monolithic integration is seriously complicated by mismatch of lattice parameters and thermal expansion coefficients between detector materials of interest and the Si substrate.

We have recently shown a novel method to grow a crack- and defect-free crystalline Ge absorber onto a Si substrate despite the large lattice (4.2 %) and thermal (130 %) mismatches [1]. It consists of fast epitaxial deposition onto Si substrates deeply patterned at a micron scale in the form of “pillars”, leading to arrays of closely spaced Ge crystals up to dozens of microns in height.

Following last year's oral presentation at the MaP symposium, we will present the recent progress in substrate fabrication and wet chemical post-growth etchings of our structures. It includes the electrical characterization of hetero-junction diodes formed by the p-Ge crystals on an n-Si substrate, with very high surface-to-volume ratios compared to the

regular, film-based Si-Ge diodes. The individual Ge crystals with various top surface morphologies were electrically contacted on their top by means of conductive micro-manipulators operating inside an SEM. Our micron-sized diodes exhibit reverse dark-currents below 1 mA/cm^2 at -10 V, which compare favourably with existing Si-Ge diodes and are promising for the development of a novel X-ray detector. Various surface treatments such as thermal oxidation help reducing the reverse dark-current [2].

[1] C.V. Falub et al., *Science* **335**, 1330 (2012). [2] T. Kreiliger et al., *Phys. Status Solidi A* **211**(1), 131 (2014).

56-B Enzyme Immobilization with a Dendronized Polymer for Surface-Localized Cascade Reactions

Andreas Küchler, A.D. Schlüter and P. Walde

Polymer Chemistry, D-MATL

A polycationic second generation dendronized polymer (denpol) was decorated in aqueous solution along the denpol chain with either *Aspergillus niger* glucose oxidase (GOD) or horseradish peroxidase (HRP) through stable covalent bis-aryl hydrazone linking units between the denpol and the enzymes. These denpol-enzyme conjugates were then adsorbed onto various SiO_2 surfaces for a two enzyme cascade reaction: Oxidation of D-glucose with GOD and dissolved O_2 yielding glucono-δ-lactone and H_2O_2, followed by oxidation of 2,2'-azinobis(3-ethylbenzothiazoline-6-sulfonate) ($ABTS^{2-}$) to $ABTS^{\bullet-}$ catalyzed by HRP and the formed H_2O_2. Based on adsorption measurements with the transmission interferometric adsorption sensor (TInAS) and based on enzymatic activity measurements it was shown that the adsorbed conjugates remained bound to the surface and that the enzymes were stable during storage. During operation, the activity was preserved for at least several hours. Overall, these denpol-enzyme conjugates allow a simple and efficient enzyme immobilization even in thin glass tubes in a single immobilization step. It was also demonstrated that not only a sequential immobilization of GOD and HRP is possible, but also a co-immobilization of the two enzymes *via* the preparation and adsorption of a conjugate carrying GOD as well as HRP along the same denpol chain.

57-C Multiscale Modelling of the Rheology of Complex Interfaces

Alan Luo, P. Ilg, L. Sagis and H.C. Oettinger

Polymer Physics, D-MATL

There is much interest in anisotropic particles adsorbed onto fluid-fluid interfaces in the context of self-assembly, surface rheology of particle-stabilised interfaces, e.g. Pickering emulsions as well as active nematics. We are interested in surface rheology, when the fluid-fluid interface has a microstructure formed by the anisotropic particles, a so-called complex interface. As a first approximation, we model anisotropic particles by hard ellipsoids and neglect capillary interactions.
Non-equilibrium thermodynamic frameworks are a promising route to developing models of mechanical behaviour for many varied systems. The particular framework we use called GENERIC [1] consists of four building blocks, which are functions of the state variables of the system we want to describe. The GENERIC building blocks are the energy, entropy, Poisson matrix and friction matrix, which must satisfy certain properties [1]. Those properties guarantee thermodynamic consistency of the system's time evolution.
We employ Monte-Carlo simulations and theoretical calculations of a hard ellipse system in order to help guide the model development and extract functional forms of the building blocks. Using these, we construct a model to describe the rheology of fluid-fluid interfaces with adsorbed anisotropic particles. We explore the behaviour of our model under various flow conditions: simple shear, oscillatory shear and dilatational shear.

[1] H.C. Oettinger, Beyond Equilibrium Thermodynamics (2005).

58-B Thermochemical Separation of Oxygen from Inert Gas via Perovskite-Based Redox Cycles Utilizing Solar Waste Heat

Miriam Ezbiri, K.M. Allen, R. Michalsky and A. Steinfeld

Renewable Energy Carriers, D-MAVT, Paul Scherrer Institute

The solar thermochemical splitting of H_2O and CO_2 by metal oxide redox cycles often makes use of inert gas during the thermal reduction to shift the thermodynamic equilibrium to lower operating temperatures and to avoid re-oxidation by quenching and dilution [1-3]. The outflowing inert gas contains thus oxygen and its recycling introduces an energy penalty in the overall process. This project seeks to thermochemically separate dilute oxygen from inert gas using waste heat derived from the solar reactor. This is achieved via a parallel redox cycle [4], this

time using nonstoichiometric perovskite materials that are thermally reduced in air at temperatures below 600°C and subsequently re-oxidized with the oxygen-containing inert gas stream. The screening of promising perovskite candidates is carried out by a combined computational-experimental approach, utilizing density functional theory (DFT) and validating with thermogravimetric analysis.

[1] J. Scheffe and A. Steinfeld, *Energ. Fuel* **26,** 1928–1936 (2012). [2] P. Loutzenhiser and A. Steinfeld, *Int. J. Hydrogen Energ* **36**, 12141-12147 (2011). [3] D. Gstoehl et al., *J. Mater. Sci.* **43**(14), 4729–4736 (2008). [4] M. Hänchen et al., *Ind. Eng. Chem. Res.* **51**(20), 7013–7021 (2012).

59-A Rejuvenation of Silicon Nanomechanical Resonators

Ye Tao, P. Navaretti, R. Hauert, U. Grob, M. Poggio and C.L. Degen

Spin Physics and Imaging, D-PHYS

We report on variable-temperature mechanical dissipation measurements carried out on thin (120 nm), single-crystal silicon cantilevers with varying chemical surface termination. We find that the 1-2 nm thick native oxide layer of silicon contributes up to 90% of the friction of the mechanical resonance. We show that the mechanical friction is proportional to the thickness of the oxide layer, and that it crucially depends on oxide formation conditions. We further demonstrate that chemical surface protection by nitridation, liquid-phase hydro-silylation or gas-phase hydrosilylation can inhibit the rapid (minutes) oxide formation in ambient air, and result in a permanent improvement of the mechanical quality factor Q of x2-x5 at room and cryogenic temperatures. Presented recipes can be directly integrated with standard cleanroom processes and may be especially beneficial for ultrasensitive nanomechanical force- and mass sensors including silicon cantilevers, membranes or nanowires.

60-C Realization of a Topological Semimetal in a Crystal with Preserved Time-Reversal Symmetry

Tomas Bzdusek, A. Rüegg and M. Sigrist

Strongly Correlated Electrons, D-PHYS

Topological phases became a topic of intense research in recent years. They show certain degree of universal behavior, which is robust against various perturbations. The most prominent example is the quantum Hall effect that exhibits an integer Hall conductivity, this property being remarkably insusceptible to the presence of disorder.

Topological semimetals are another example of a topological phase. Their electronic structure is gapped everywhere except for a discrete set of momenta, the so-called Weyl nodes. These points constitute the bulk Fermi surface and their presence is robust against weak perturbations. Topological semimetals exhibit a non-trivial surface states that are characterized by a set of open Fermi arcs instead of closed Fermi lines.

In our work we study a tight-binding model of non-interacting spin-orbit coupled electrons moving in an elastic pyrochlore lattice. If the filling factor is set to either 1/4 or 3/4 and the crystal elasticity is large, the electrons can form a semimetal that contains a graphene-like Dirac nodes. If the elasticity is decreased below a critical value, a spontaneous Peierls type transition occurs that is accompanied by splitting each Dirac node into multiple Weyl nodes, thus leading to a topological phase.

Contrary to the mostly studied case, this realization of a topological semimetal preserves time-reversal symmetry and breaks parity. We observe that the topology of the Fermi arcs depends on the termination of the crystal. The various terminations can be connected by an adiabatic evolution of the Hamiltonian. We inspect the Lifshitz type of transition that occurs during such evolution and that preserves the topology of the bulk.

61-A Controlled Growth and Interfaces of Supported Iridium Nanoparticles via Surface Organometallic Chemistry

Florent Héroguel, G. Siddiqi, O. Safonova, M.D. Detwiler, D.Y. Zemlyanov and C. Copéret

Surface and Interfacial Chemistry, D-CHAB

Aluminosilicates are the most used catalysts and catalyst supports. Together with metal nanoparticles, amorphous silica-aluminas (ASA) provide bi-functional catalysts, which exploit the mild acidity of ASA and the hydrogenation/hydrogenolysis properties of metal nanoparticles.

In this study, we apply the concepts of Surface Organometallic Chemistry (SOMC) to the controlled growth of iridium nanoparticles on silica and alumina. On the latter, the metal-support interface is tuned upon decomposition of a well-defined dimeric supported iridium siloxide, with the formation of a silicon aluminate layer conferring mild acidity to the materials. The particles display all the desired properties for applications in catalysis, thanks to the use of organometallic precursors: they are small (0.5 nm), narrowly dispersed, with a homogeneous spatial distribution and the absence of large metal aggregates and pollution of the metal surface with residual ligands

We present the synthesis of the materials as well as their detailed characterization at every step using molecular and surface science techniques such as NMR and FTIR spectroscopies, TEM, XAS, XPS, as well as chemisorption. Finally, catalytic results probing the materials bifunctionality are discussed.

62-C From Nano to Micro, a Challenge in Bridging Scales

Clément V.M. Cremmel, L. Isa and N.D. Spencer

Surface Science and Technology, D-MATL

The osseointegration of titanium implants is known to be significantly influenced by their surface roughness. This surface property has a significant influence on cell behaviour, such as adhesion, proliferation and differentiation. In order to investigate the effect of roughness on cell attachment, roughness gradients offer an ideal, high-throughput solution [1].
While previous studies [2] showed a higher osteoblast proliferation on micrometer-sized roughness compared to flat references, nanometer-scale roughness was shown to slow down cell proliferation [3, 4]. In order to understand the effect of roughness scale on the behavior of osteoblasts, new particle-size gradients are currently being developed.
Three new techniques have been investigated. First, the oxidation of organic particles through UV illumination was used to generate particle-height gradients. Secondly, separation and deposition of a polydisperse particle suspension was performed by means of an electric field in an acrylamide gel. The preparation of such polydisperse silica-particle suspensions required a significant adaptation of the well-known Stöber synthesis. Finally, silver layers were deposited with varying thicknesses on silicon wafers, followed by dewetting at 600°C, to fabricate a particle-size gradient, with features in a range of 300 nm to 5 nm.

[1] S. Morgenthaler et al., *Soft Matter* **4**(3), 419-434 (2008). [2] T.P. Kunzler et al., *Biomaterials* **28**(13), 2175-2182 (2007). [3] C. Huwiler et al., *Langmuir* **23**(11), 5929-5935 (2007). [4] T.P. Kunzler et al., *Biomaterials* **28**(33), 5000-5006 (2007).

63-B A Novel Setup for Measuring Solvent Permeability in Lubricating Polymer-Brush Coatings

Christian Mathis, L. Isa and N.D. Spencer

Surface Science and Technology, D-MATL

Research on polymer brushes, grafted polymer chains densely grown on a surface, has enjoyed growing attention in recent years due to their enormous potential for friction reduction in industrial as well as medical applications. Well-designed polymer-brush coatings, with thickness in the nanometer range, possess the ability to reduce friction beyond theoretically expected values [1]. However, the details of the lubrication mechanisms and the interplay with the confinement of liquid within the polymer-brush system, are yet to be fully explained [2]. The aim of this project is to shed light on these phenomena by investigating the role of confined fluids in the lubrication mechanisms via the measurement of the permeability of the viscous fluid flow through polymer-brushes.
A novel experimental microfluidic setup is currently being developed. The aim is to derive the permeability value from the pressure drop across micrometric channels filled with the polymer brushes, as a function of flow rates. Varying the solvent quality as well as the polymer brush grafting density will elucidate the interaction between fluid and solid brush structure. Furthermore, brush permeability in squeeze flows will be characterized by means of AFM indentation experiments and will be compared to the outcome of the microfluidics experiments.

[1] R.M. Bielecki et al., *Tribol. Lett.* **49**, 263–272 (2012). [2] R.M. Espinosa-Marzal et al., *Soft Matter* **9**, 10572–10585 (2013).

64-A Limiting Mechanism for Critical Current in Topologically Frustrated Josephson Junctions in Sr_2RuO_4

Sarah Etter, H. Kaneyasu, M. Ossadnik and M. Sigrist

Theoretical Physics, D-PHYS

We study a Josephson junction of cylindrical geometry between a conventional *s*-wave and a chiral *p*-wave superconductor. Such junctions appear naturally in eutectic Sr_2RuO_4-Ru. Depending on temperature, two different superconducting phases are realized at the interface. While one leads to a conventional Josephson effect, the other is topologically frustrated which profoundly changes its behavior due to the appearance of a spontaneous flux pattern involved in a pinning-depinning transition. We discuss in detail this new limiting mechanism for the critical current in the frustrated case and compare it to the conventional case. Our results are relevant to explain anomalous features observed in Pb/Ru/Sr_2RuO_4 junctions in recent experiments by Maeno *et al*.

65-C Simulation of the Evolution of the Yield Locus of Deep Drawing Steel by Means of Crystal Plasticity

Christian Raemy, B. Berisha and P. Hora

Virtual Manufacturing, D-MAVT

The present study aimed to obtain macroscopic material properties based on microscopic simulations, since the necessary laboratory experiments (e.g. biaxial compression test) are difficult to conduct. Two numerical strategies, the finite element method and a so called spectral solver were compared. Since the spectral solver, provided by the open source crystal plasticity software package DAMASK, turned out to be better suited, this method was used to approach the problem.
The texture of cold rolled deep drawing steel DC05 was measured and the orientation distribution function (ODF) was calculated. A small number (25) of representative orientations with their respective volume fraction was determined and a model of a representative volume element (RVE) was created, reproducing a microstructure with these orientations, distributed to 39 grains.
An optimization was conducted to fit the parameters of a simple crystal plasticity constitutive model, such that the simulated flow curve of this RVE matches the measured flow curve of the sheet metal of which the ODF was gained.
Several simulations of biaxial plane stress states with different stress ratios were performed in order to determine the yield stresses in rolling and transverse direction of the sheet at different points of the yield locus. A similar proceeding was performed after the RVE was virtually prestrained by 15% in rolling direction.
The results were compared to newest macroscopic models for the prediction of the anisotropic strain hardening of materials undergoing nonlinear strain paths. It was found, that the examined virtual model predicts the deformation of the yield locus in a qualitatively comparable manner. Hence, the applied method is able to link microscopic with macroscopic phenomena. Future work will be focused on the incorporation of additional input data based on experiments (e.g. measurement of dislocation density) in order to improve the prediction capability of the microscopic model.

66-B A PDMS-Based Strain Sensor

Giuseppe Cantarella, N. Münzenrieder, L. Petti, C. Vogt, L. Büthe, G. Salvatore and G. Tröster

Wearable Computing, D-ITET

In the last years, researchers have been interested in the development of stretchable sensors for several applications, such as artificial skin. These devices are daily used and have to be low-cost. Here, it is reported the fabrication and performances of a strain sensor based on Polydimethylsiloxane (PDMS). PDMS is a silicon-based organic polymer, which is suitable for electronic skin thanks to its mechanically flexible and biocompatible nature. The fabrication process consists of spin coating 50 nm water-dissolvable layer of Polyvinyl alcohol (PVA) and 100 μm PDMS on a Si substrate. An oxygen plasma treatment of the organic polymer is required in order to guarantee a surface roughness $\approx$ 2 nm and then evaporation of 10 nm Titanium (for improve adhesion) and 60 nm of Gold is done. Later, the PDMS layer is released by dissolving the PVA layer in water. Experimental results show how mechanical strain of 10% increases the electrical resistance by a factor of 27. Whereas, for strain > 10%, metal cracks are visible, no conductivity occurs. In this research, good mechanical and electrical properties together with the biocompatibility of PDMS show how this sensor can have an important role in future biomedical applications.

67-A Micro Optical Bench for Textile Integrated MRI Data Links

Christian Vogt, L. Büthe, N. Münzenrieder, L. Petti, G. Cantarella and G. Tröster

Wearable Computing, D-ITET

Textile integrated electronics provide unobtrusive measurements of people's health, for example by measuring their heart rate, body temperature or posture. Further health applications are magnetic resonance imaging (MRI), where electronic textiles would improve measurement quality and patient comfort. Magnetic field strengths beyond 3 Tesla and radio frequency pulses in the kilo-Watt range provide new challenges for such e-textiles. Traditionally, measurement data is transferred via coaxial cables in MRI. In contrast, glass fibers would provide EM immunity and low signal loss for this data transmission. Therefore, a micro optical bench (MOB) to couple a glass fiber to a laser diode small enough to be woven into a textile is realized by spincoating 12 μm of SU-8 on a silicon wafer and subsequent photolithographic patterning of an opening to attach a laser diode. Afterwards a 100 μm SU-8 sheet is spincoated on top of the first one and patterned with a 130 μm groove to be used as a guide for the glass fiber. After dicing of the wafer, these MOBs with a size of 1.5 mm x 0.7 mm are used to connect the output of the laser diode to a glass fiber by employing the capillary forces of an adhesive for self-aligning the fiber with respect to the groove and laser diode. This method aligns the fiber within 1.86 μm in horizontal and 0.47 μm in vertical direction inside the groove. The overall light coupling efficiency from the laser to fiber coupling is measured to be 76%. Based on this laser to fiber

coupling a data link with a transfer rate of 1Gbit/s was realized.

68-C Copper Coating of Wood Structures

Jana Segmehl, V. Merk, M. Chanana and I. Burgert

Wood Materials Science, D-BAUG

Copper nano-particles have been introduced into the hierarchical structure of spruce and beech wood following the procedure for liquid phase deposition of copper thin films recently published by Kraenzlin et al. [1]. SEM Investigations revealed both, a narrow particle size distribution as well as a homogeneous distribution of the particles in the wood structure. XRD and EDX measurements confirmed that the formed metallic face is Cu (0).
The functionalization of wood by the deposition of copper nano coatings at various grades and qualities by variation of precursor concentration and annealing procedures can result in advanced wood applications. The enhancement of electrical conductivity, the applicability of wood as a storage medium for gaseous species and in catalysis technology as well as the preparation of replica and free standing metallic foams are potential fields of implementation.

[1] N. Kränzlin et al., *Angew. Chem. Int. Ed.* **51**, 19, 4743-4746 (2012).

LIST OF PARTICIPANTS

Antonini Carlo, Dr., *Thermodynamics in Emerging Technologies, D-MAVT, ETH Zurich*, carlo.antonini@mavt.ethz.ch
Bargardi Fabio, *D-MATL, ETH Zurich*, fabioba@student.ethz.ch
Becher Carsten, *Multifunctional Ferroic Materials, D-MATL, ETH Zurich*, carsten.becher@mat.ethz.ch
Bernoulli Daniel, *Nanometallurgy, D-MATL, ETH Zurich*, daniel.bernoulli@mat.ethz.ch
Blattmann Christoph, *Particle Technology Laboratory, D-MAVT, ETH Zurich*, blattmac@student.ethz.ch
Boenzli Eva, Dr., *Bioanalytics Group, D-CHAB, ETH Zurich*, eva.boenzli@org.chem.ethz.ch
Bolisetty Sreenath, Dr., *Food and Soft Materials, D-HEST, ETH Zurich*, sreenath.bolisetty@hest.ethz.ch
Böni Lukas, *Food Process Engineering, D-HEST, ETH Zurich*, boenil@student.ethz.ch
Bran Anleu Paula, *Physical Chemistry of Building Materials, D-BAUG, ETH Zurich*, pbran@ethz.ch
Bräunlich Irene, *Polymer Technology, D-MATL, ETH Zurich*, irene.braeunlich@mat.ethz.ch
Brechbuehl Sonia, *D-MATL, ETH Zurich*, soniabr@student.ethz.ch
Brenner Oliver, *Particle Technology Laboratory, D-MAVT, ETH Zurich*, brennero@student.ethz.ch
Broguiere Nicolas, *Cartilage Engineering and Regeneration, D-HEST, ETH Zurich*, nicolas.broguiere@hest.ethz.ch
Büchel Robert, Dr., *Particle Technology Laboratory, D-MAVT, ETH Zurich*, buechel@ptl.mavt.ethz.ch
Büchi Jonathan, *D-MATL, ETH Zurich*, buechij@student.ethz.ch
Burgert Ingo, Prof., *Wood Materials Science, D-BAUG, ETH Zurich*, iburgert@ethz.ch
Busato Stephan, Dr., *Polymer Technology, D-MATL, ETH Zurich*, sbusato@ethz.ch
Büthe Lars, *Wearable Computing, D-ITET, ETH Zurich*, lars.buethe@ife.ee.ethz.ch
Bzdusek Tomas, *Strongly Correlated Electrons, D-PHYS, ETH Zurich*, tbzduek@phys.ethz.ch
Cantarella Giuseppe, *Wearable Computing, D-ITET, ETH Zurich*, giuseppe.cantarella@ife.ee.ethz.ch
Carnelli Davide, Dr., *Complex Materials, D-MATL, ETH Zurich*, davide.carnelli@mat.ethz.ch
Caruso Francesco, Dr., *Physical Chemistry of Building Materials, D-BAUG, ETH Zurich*, fcaruso@ethz.ch
Cerqua Simon, *Polymer Chemistry, D-MATL, ETH Zurich*, simon.cerqua@mat.ethz.ch
Chen Philipp, *Complex Materials, D-MATL, ETH Zurich*, philipp.chen@mat.ethz.ch
Cheng Jason, Prof., *Visiting Professor from University of California Riverside at Biosensors and Bioelectronics, D-ITET*, cheng@biomed.ee.ethz.ch
Chikkadi Kiran, Dr., *Micro and Nanosystems, D-MAVT, ETH Zurich*, kiranc@ethz.ch
Courty Diana, Dr., *Nanometallurgy, D-MATL, ETH Zurich*, diana.courty@mat.ethz.ch
Cremmel Clément V.M., *Surface Science and Technology, D-MATL, ETH Zurich*, clement.cremmel@mat.ethz.ch
Dasargyri Athanasia, *Drug Formulation and Delivery, D-CHAB, ETH Zurich*, athanasia.dasargyri@pharma.ethz.ch
de Lange Victoria, *Biosensors and Bioelectronics, D-ITET, ETH Zurich*, delange@biomed.ee.ethz.ch
De Leo Eva, *Optical Materials Engineering, D-MAVT, ETH Zurich*, deleoe@ethz.ch
Dedisse Anne-Juliette, *Food and Soft Materials, D-HEST, ETH Zurich*, anne-juliette.dedisse@epfl.ch
Deffner Bernd, *Polymer Chemistry, D-MATL, ETH Zurich*, bernd.deffner@mat.ethz.ch
Delpero Tommaso, *Composite Materials and Adaptive Structures, D-MAVT, ETH Zurich*, tdelpero@ethz.ch
Di Fratta Claudio, *Composite Materials and Adaptive Structures, D-MAVT, ETH Zurich*, claudiodifratta@mavt.ethz.ch
Dittrich Petra S., Prof., *Bioanalytics Group, D-CHAB, ETH Zurich*, dittrich@org.chem.ethz.ch
Döring Valentin, *Micro and Nanosystems, D-MAVT, ETH Zurich*, vdoering@ethz.ch
Durrer Lukas, Dr., *Micro and Nanosystems, D-MAVT, ETH Zurich*, lukas.durrer@micro.mavt.ethz.ch
Dymkowski Krzysztof, *Materials Theory, D-MATL, ETH Zurich*, krzysztof.dymkowski@mat.ethz.ch
Eller Jens, Dr., *Nanoelectronics, D-ITET, ETH Zurich*, jens.eller@iis.ee.ethz.ch
Erdem Derya, *Multifunctional Materials, D-MATL, ETH Zurich*, derya.erdem@mat.ethz.ch
Etter Sarah, *Theoretical Physics, D-PHYS, ETH Zurich*, etters@itp.phys.ethz.ch
Etterlin Gion Diego, *Particle Technology Laboratory, D-MAVT, ETH Zurich*, gione@ethz.ch
Ezbiri Miriam, *Renewable Energy Carriers, D-MAVT, Paul Scherrer Institute*, miriam.ezbiri@psi.ch
Fedorova Natalya, *Materials Theory, D-MATL, ETH Zurich*, natalya.fedorova@mat.ethz.ch
Ferguson Stephen, Prof., *Biomechanics, D-HEST, ETH Zurich*, sferguson@ethz.ch
Fischer Peter, Prof., *Food Process Engineering, D-HEST, ETH Zurich*, pefi@ethz.ch
Fong Wye Khay, Dr., *Food and Soft Materials, D-HEST, ETH Zurich*, khay.fong@hest.ethz.ch

Formica Florian, *Cartilage Engineering and Regeneration, D-HEST, ETH Zurich*, florian.formica@hest.ethz.ch
Gauthier Nicolas, *Laboratory of Developments and Methods, D-PHYS, Paul Scherrer Institute*, nicolas.gauthier@psi.ch
Gelardi Giulia, *Physical Chemistry of Building Materials, D-BAUG, ETH Zurich*, gelardig@ethz.ch
Ghanbari Reza, *Food and Soft Materials, D-HEST, ETH Zurich*, reza.ghanbari@hest.ethz.ch
Glauser Oliver, *Physical Chemistry of Building Materials, D-BAUG, ETH Zurich*, glausero@ethz.ch
Gong Yuhui, *Drug Formulation and Delivery, D-CHAB, ETH Zurich*, yuhui.gong@pharma.ethz.ch
Goren Tolga, Dr., *Surface Science and Technology, D-MATL, ETH Zurich*, tolga.goren@gmail.com
Goudeli Eirini, *Particle Technology Laboratory, D-MAVT, ETH Zurich*, goudeli@ptl.mavt.ethz.ch
Gröhn Arto, *Particle Technology Laboratory, D-MAVT, ETH Zurich*, arto.groehn@ptl.mavt.ethz.ch
Grossman Madeleine, *Complex Materials, D-MATL, ETH Zurich*, madeleine.grossman@mat.ethz.ch
Grüning Wolfram, *Surface and Interfacial Chemistry, D-CHAB, ETH Zurich*, gruening@inorg.chem.ethz.ch
Gstrein Chiara, *Polymer Chemistry, D-MATL, ETH Zurich*, chiara.gstrein@mat.ethz.ch
Güntner Andreas, *Particle Technology Laboratory, D-MAVT, ETH Zurich*, andreas.guentner@ptl.mavt.ethz.ch
Gyr Raphael, *D-MATL, ETH Zurich*, raphael.gyr@mat.ethz.ch
Haberl Johannes, Dr., *Food and Soft Materials, D-HEST, ETH Zurich*
Haluska Miroslav, Dr., *Micro and Nanosystems, D-MAVT, ETH Zurich*, haluska@micro.mavt.ethz.ch
Hassani Mohammad Masoud, *Computational Physics of Engineering Materials, D-BAUG, ETH Zurich*, Mhassani@ethz.ch
Hassanpour Yesaghi Ehsan, *Multifunctional Ferroic Materials, D-MATL, ETH Zurich*, ehsan.hassanpour@mat.ethz.ch
Heiligtag Florian, *Multifunctional Materials, D-MATL, ETH Zurich*, florian.heiligtag@mat.ethz.ch
Heinrich Michael, *Optical Materials Engineering, D-MAVT, ETH Zurich*, michahei@ethz.ch
Héroguel Florent, *Surface and Interfacial Chemistry, D-CHAB, ETH Zurich*, florenth@student.ethz.ch
Hierold Christofer, Prof., *Micro and Nanosystems, D-MAVT, ETH Zurich*, hierold@micro.mavt.ethz.ch
Hirsch Ofer, *Multifunctional Materials, D-MATL, ETH Zurich*, ofer.hirsch@mat.ethz.ch
Hitzbleck Martina, Dr., *Biosensors and Bioelectronics, D-ITET, ETH Zurich*
Janis Vinklers, *Energy Conversion, D-MAVT, ETH Zurich*, vinklers@lec.mavt.ethz.ch
Jordens Sophia, *Food and Soft Materials, D-HEST, ETH Zurich*, sophia.jordens@hest.ethz.ch
Junesch Juliane, *Biosensors and Bioelectronics, D-ITET, ETH Zurich*, junesch@biomed.ee.ethz.ch
Kakeru Fujiwara, *Particle Technology Laboratory, D-MAVT, ETH Zurich*, fujiwara@ptl.mavt.ethz.ch
Kandemir Ayse Cagil, *Nanometallurgy, D-MATL, ETH Zurich*, ayse.oezkaraca@mat.ethz.ch
Kelesidis Georgios, *Particle Technology Laboratory, D-MAVT, ETH Zurich*, kelesidg@ethz.ch
Kesti Matti, *Cartilage Engineering and Regeneration, D-HEST, ETH Zurich*, matti.kesti@hest.ethz.ch
Koirala Rajesh, *Particle Technology Laboratory, D-MAVT, ETH Zurich*, rkoirala@ptl.mavt.ethz.ch
Kokkinis Dimitri, *Complex Materials, D-MATL, ETH Zurich*, dimitri.kokkinis@mat.ethz.ch
Koren Vitaly, *Particle Technology Laboratory, D-MAVT, ETH Zurich*, vikoren@ethz.ch
Kory Max, *Polymer Chemistry, D-MATL, ETH Zurich*, max.kory@mat.ethz.ch
Kreiliger Thomas, *Physics of New Materials, D-PHYS, ETH Zurich*, thomaskr@phys.ethz.ch
Küchler Andreas, *Polymer Chemistry, D-MATL, ETH Zurich*, akuechler@mat.ethz.ch
Kurlov Alexey, *Energy Science and Engineering, D-MAVT, ETH Zurich*, kurlova@student.ethz.ch
Lagadec Marie Francine, *Nanoelectronics, D-ITET, ETH Zurich*, lagadec@iis.ee.ethz.ch
Läubli Nino, *Multi-Scale Robotics, D-MAVT, ETH Zurich*, laeublin@student.ethz.ch
Le Ferrand Hortense, *Complex Materials, D-MATL, ETH Zurich*, hortense.leferrand@mat.ethz.ch
Leibacher Ivo, *Center of Mechanics, D-MAVT, ETH Zurich*, leibacher@imes.mavt.ethz.ch
Lenz Mario, *Bioanalytics Group, D-CHAB, ETH Zurich*, mario.lenz@org.chem.ethz.ch
Leo Naëmi, *Multifunctional Ferroic Materials, D-MATL, ETH Zurich*, naemi.leo@mat.ethz.ch
Leroux Jean-Christophe, Prof., *Drug Formulation and Delivery, D-CHAB, ETH Zurich*, jleroux@ethz.ch
Libanori Rafael, Dr., *Complex Materials, D-MATL, ETH Zurich*, libanori@mat.ethz.ch
Lilienblum Martin, *Multifunctional Ferroic Materials, D-MATL, ETH Zurich*, martin.lilienblum@mat.ethz.ch
Lin Weyde, *Nanoelectronics, D-ITET, ETH Zurich*, weydelin@iis.ee.ethz.ch
Liu Wei, *Micro and Nanosystems, D-MAVT, ETH Zurich*, wei.liu@micro.mavt.ethz.ch
Lloret Ena, *Architecture and Digital Fabrication, D-BAUG, ETH Zurich*, lloret@arch.ethz.ch
Louis Bryan, *Composite Materials and Adaptive Structures, D-MAVT, ETH Zurich*, blouis@mavt.ethz.ch
Luo Alan, *Polymer Physics, D-MATL, ETH Zurich*, alan.luo@mat.ethz.ch

Ma Huan, *Nanometallurgy, D-MATL, ETH Zurich*, huan.ma@mat.ethz.ch
Mantellato Sara, *Physical Chemistry of Building Materials, D-BAUG, ETH Zurich*, sara.mantellato@ifb.baug.ethz.ch
Marchon Delphine, *Physical Chemistry of Building Materials, D-BAUG, ETH Zurich*, marchond@ethz.ch
Martiel Isabelle, *Food and Soft Materials, D-HEST, ETH Zurich*, isabelle.martiel@hest.ethz.ch
Mathis Christian, *Surface Science and Technology, D-MATL, ETH Zurich*, mathisc@ethz.ch
Maurel Laura, *Multifunctional Ferroic Materials, D-MATL, ETH Zurich*, laura.maurel@mat.ethz.ch
Meng Li, *Nanoscience for Energy Technology and Sustainability, D-MAVT, ETH Zurich*, mli@student.ethz.ch
Merk Vivian, *Wood Materials Science, D-BAUG, ETH Zurich*, vmerk@ethz.ch
Mettler Linus, *Computational Physics of Engineering Materials, D-BAUG, ETH Zurich*, mettlerl@ifb.baug.ethz.ch
Mezzenga Raffaele, Prof., *Food and Soft Materials, D-HEST, ETH Zurich*, raffaele.mezzenga@hest.ethz.ch
Morgenthaler Sara, Dr., *MaP, ETH Zurich*, sara.morgenthaler@mat.ethz.ch
Morgese Giulia, *Surface Science and Technology, D-MATL, ETH Zurich*, giulia.morgese@mat.ethz.ch
Mostrou Sotiria, *Particle Technology Laboratory, D-MAVT, ETH Zurich*, smostrou@student.ethz.ch
Muff Daniel, *Nanometallurgy, D-MATL, ETH Zurich*, daniel.muff@mat.ethz.ch
Müller Claudia, *Nanometallurgy, D-MATL, ETH Zurich*, claudia.mueller@mat.ethz.ch
Munglani Gautam, *Computational Physics of Engineering Materials, D-BAUG, ETH Zurich*, gmunglani@ethz.ch
Münzenrieder Niko, Dr., *Wearable Computing, D-ITET, ETH Zurich*, muenzenrieder@ife.ee.ethz.ch
Muoth Matthias, Dr., *Micro and Nanosystems, D-MAVT, ETH Zurich*
Murer Christoph, *D-MATL, ETH Zurich*, Cmurer@student.ethz.ch
Mushtaq Fajer, *Multi-Scale Robotics, D-MAVT, ETH Zurich*, fmushtaq@student.ethz.ch
Naik Vikrant, Dr., *Surface Science and Technology, D-MATL, ETH Zurich*, vikrant.naik@mat.ethz.ch
Nasira Hoda, *Food and Soft Materials, D-HEST, ETH Zurich*, hoda.nasira@hest.ethz.ch
Nelson Adrienne, *Interfaces, Soft Matter and Assembly, D-MATL, ETH Zurich*, adrienne.nelson@mat.ethz.ch
Niebel Tobias, *Complex Materials, D-MATL, ETH Zurich*, tobias.niebel@mat.ethz.ch
Nyström Gustav, Dr., *Food and Soft Materials, D-HEST, ETH Zurich*, gustav.nystroem@hest.ethz.ch
Öztürk Ece, *Cartilage Engineering and Regeneration, D-HEST, ETH Zurich*, ece.oeztuerk@hest.ethz.ch
Pecnik Christina, *Nanometallurgy, D-MATL, ETH Zurich*, christina.pecnik@mat.ethz.ch
Pineau Nicolay, *Particle Technology Laboratory, D-MAVT, ETH Zurich*, pineaun@student.ethz.ch
Poulikakos Lisa, *Optical Materials Engineering, D-MAVT, ETH Zurich*, plisa@ethz.ch
Praticò Ylenia, *Physical Chemistry of Building Materials, D-BAUG, ETH Zurich*, praticoy@ethz.ch
Pustovgar Elizaveta, *Physical Chemistry of Building Materials, D-BAUG, ETH Zurich*, pustovge@ethz.ch
Raemy Christian, *Virtual Manufacturing, D-MAVT, ETH Zurich*, christian.raemy@ivp.mavt.ethz.ch
Reichert Peter, *Center of Mechanics, D-MAVT, ETH Zurich*, peter.c.reichert@web.de
Reiter Lex, *Physical Chemistry of Building Materials, D-BAUG, ETH Zurich*, reiter@ifb.baug.ethz.ch
Rey Marcel, *D-MATL, ETH Zurich*, mrey@student.ethz.ch
Robotti Francesco, *Thermodynamics in Emerging Technologies, D-MAVT, ETH Zurich*, robottif@ethz.ch
Röthlisberger André, *Nanometallurgy, D-MATL, ETH Zurich*, andre.roethlisberger@mat.ethz.ch
Rühs Patrick, *Food Process Engineering, D-HEST, ETH Zurich*, patrick.ruehs@hest.ethz.ch
Saha Abhijit, Dr., *Food and Soft Materials, D-HEST, ETH Zurich*, abhijit.saha@hest.ethz.ch
Sampethai Sofia, *Particle Technology Laboratory, D-MAVT, ETH Zurich*, sasofia@student.ethz.ch
Sanabria Sergio, Dr., *Wood Physics, D-BAUG, ETH Zurich*, ssanabria@ethz.ch
Sanchez-Ferrer Antoni, Dr., *Food and Soft Materials, D-HEST, ETH Zurich*, antoni.sanchez@hest.ethz.ch
Sangiorgio Boris, *Materials Theory, D-MATL, ETH Zurich*, boris.sangiorgio@mat.ethz.ch
Schaab Jakob, *Multifunctional Ferroic Materials, D-MATL, ETH Zurich*, jakob.schaab@mat.ethz.ch
Schaffner Manuel, *Complex Materials, D-MATL, ETH Zurich*, schamanu@ethz.ch
Schefer Larissa, *Food and Soft Materials, D-HEST, ETH Zurich*, larissa.schefer@hest.ethz.ch
Schlich Franziska, *Nanometallurgy, D-MATL, ETH Zurich*, franziska.schlich@mat.ethz.ch
Schönherr Peggy, *Multifunctional Ferroic Materials, D-MATL, ETH Zurich*, peggy.schoenherr@mat.ethz.ch
Schweiger Sebastian, *Electrochemical Materials, D-MATL, ETH Zurich*, sebastian.schweiger@mat.ethz.ch
Schwenke Konrad, *Microstructure and Rheology of Building Materials, D-BAUG, ETH Zurich*, konrasch@ethz.ch

Segmehl Jana, *Wood Materials Science, D-BAUG, ETH Zurich*, jsegmehl@ethz.ch
Seguí Femenias Yurena, *Physical Chemistry of Building Materials, D-BAUG, ETH Zurich*, syurena@ethz.ch
Serc Leon, *Polymer Chemistry, D-MATL, ETH Zurich*, leon.serc@mat.ethz.ch
Shen Yi, *Food and Soft Materials, D-HEST, ETH Zurich*, yi.shen@hest.ethz.ch
Sommer Marianne, *Complex Materials, D-MATL, ETH Zurich*, marianne.sommer@mat.ethz.ch
Songbo Ni, *Interfaces, Soft Matter and Assembly, D-MATL, ETH Zurich*, songbo.ni@mat.ethz.ch
Spadaro Fabiana, *Surface Science and Technology, D-MATL, ETH Zurich*, fabiana.spadaro@mat.ethz.ch
Speziale Chiara, *Food and Soft Materials, D-HEST, ETH Zurich*, chiara.speziale@hest.ethz.ch
Spolenak Ralph, Prof., *Nanometallurgy, D-MATL, ETH Zurich*, ralph.spolenak@mat.ethz.ch
Spyrogianni Anastasia, *Particle Technology Laboratory, D-MAVT, ETH Zurich*, spyrogianni@ptl.mavt.ethz.ch
Sridhar Manasa, *Heterogeneous Catalysis, D-CHAB, ETH Zurich*, manasa.sridhar@psi.ch
Staniuk Malwina, *Multifunctional Materials, D-MATL, ETH Zurich*, malwina.staniuk@mat.ethz.ch
Starsich Fabian, *Particle Technology Laboratory, D-MAVT, ETH Zurich*, fabiasta@ethz.ch
Stauffer Flurin, *Biosensors and Bioelectronics, D-ITET, ETH Zurich*, stauffer@biomed.ee.ethz.ch
Stefanoni Matteo, *Physical Chemistry of Building Materials, D-BAUG, ETH Zurich*, matteost@ethz.ch
Stratz Simone, *Bioanalytics Group, D-CHAB, ETH Zurich*, Simone.Stratz@org.chem.ethz.ch
Stucki Mario, *Functional Materials Laboratory, D-CHAB, ETH Zurich*, mario.stucki@chem.ethz.ch
Studart André, Prof., *Complex Materials, D-MATL, ETH Zurich*, andre.studart@mat.ethz.ch
Sun Wenjie, *Food and Soft Materials, D-HEST, ETH Zurich*, wenjie.sun@hest.ethz.ch
Suraneni Prannoy, *Physical Chemistry of Building Materials, D-BAUG, ETH Zurich*, psuraneni@ethz.ch
Tagliabue Giulia, *Thermodynamics in Emerging Technologies, D-MAVT, ETH Zurich*, giuliat@ethz.ch
Tanno Alexander, *Biosensors and Bioelectronics, D-ITET, ETH Zurich*, tanno@biomed.ee.ethz.ch
Tao Ye, *Spin Physics and Imaging, D-PHYS, ETH Zurich*, ytao@phys.ethz.ch
Tervoort Theo, Dr., *Polymer Technology, D-MATL, ETH Zurich*, theo.tervoort@mat.ethz.ch
Tiefenauer Raphael, *Biosensors and Bioelectronics, D-ITET, ETH Zurich*, tiefenauer@biomed.ee.ethz.ch
Usov Ivan, *Food and Soft Materials, D-HEST, ETH Zurich*, ivan.usov@hest.ethz.ch
Vallooran Jijo, *Food and Soft Materials, D-HEST, ETH Zurich*, jijo.vallooran@hest.ethz.ch
Verboket Pascal Emilio, *Bioanalytics Group, D-CHAB, ETH Zurich*, Pascal.Verboket@org.chem.ethz.ch
Vogt Christian, *Wearable Computing, D-ITET, ETH Zurich*, christian.vogt@ife.ee.ethz.ch
vom Stein Helena, *Interfaces, Soft Matter and Assembly, D-MATL, ETH Zurich*, vhelena@student.ethz.ch
Walde Peter, Prof., *Polymer Chemistry, D-MATL, ETH Zurich*, peter.walde@mat.ethz.ch
Walser Jochen, *Biomechanics, D-HEST, ETH Zurich*, jowalser@ethz.ch
Wangler Timothy, Dr., *Physical Chemistry of Building Materials, D-BAUG, ETH Zurich*, wangler@ifb.baug.ethz.ch
Waser Oliver, *Particle Technology Laboratory, D-MAVT, ETH Zurich*, oliver.waser@ptl.mavt.ethz.ch
Wegner Karsten, Dr., *Particle Technology Laboratory, D-MAVT, ETH Zurich*, wegner@ptl.mavt.ethz.ch
Wegscheider Werner, Prof., *Advanced Semiconductor Quantum Materials, D-PHYS, ETH Zurich*, werner.wegscheider@phys.ethz.ch
Wetli Christoph, *Multifunctional Ferroic Materials, D-MATL, ETH Zurich*, christoph.wetli@mat.ethz.ch
Wyss Andi, *Nanometallurgy, D-MATL, ETH Zurich*, andi.wyss@mat.ethz.ch
Yanuo Shi, *Electrochemical Materials, D-MATL, ETH Zurich*, yanuo.shi@mat.ethz.ch
Yazdani Nuri, *Nanoelectronics, D-ITET, ETH Zurich*, nuri@ethz.ch
Yu Hao, *Polymer Chemistry, D-MATL, ETH Zurich*, hao.yu@mat.ethz.ch
Zahn Raphael, Dr., *Biosurfaces Unit, CIC BiomaGUNE, San Sebastian, Spain*, rzahn@cicbiomagune.es
Zambelli Tomaso, Dr., *Biosensors and Bioelectronics, D-ITET, ETH Zurich*, zambelli@biomed.ee.ethz.ch
Zanini Michele, *Interfaces, Soft Matter and Assembly, D-MATL, ETH Zurich*, michele.zanini@mat.ethz.ch
Zeng Guobo, *Multifunctional Materials, D-MATL, ETH Zurich*, guobo.zeng@mat.ethz.ch
Zenobi Marcy, Prof., *Cartilage Engineering and Regeneration, D-HEST, ETH Zurich*, zmarcy@ethz.ch
Zhang Baozhong, Dr., *Polymer Chemistry, D-MATL, ETH Zurich*, baozhong.zhang@mat.ethz.ch
Zhao Jianguo, *Food and Soft Materials, D-HEST, ETH Zurich*, jianguo.zhao@hest.ethz.ch
Zheng Zhikun, Dr., *Polymer Chemistry, D-MATL, ETH Zurich*, zhikun.zheng@mat.ethz.ch
Zou Yu, *Nanometallurgy, D-MATL, ETH Zurich*, yu.zou@mat.ethz.ch

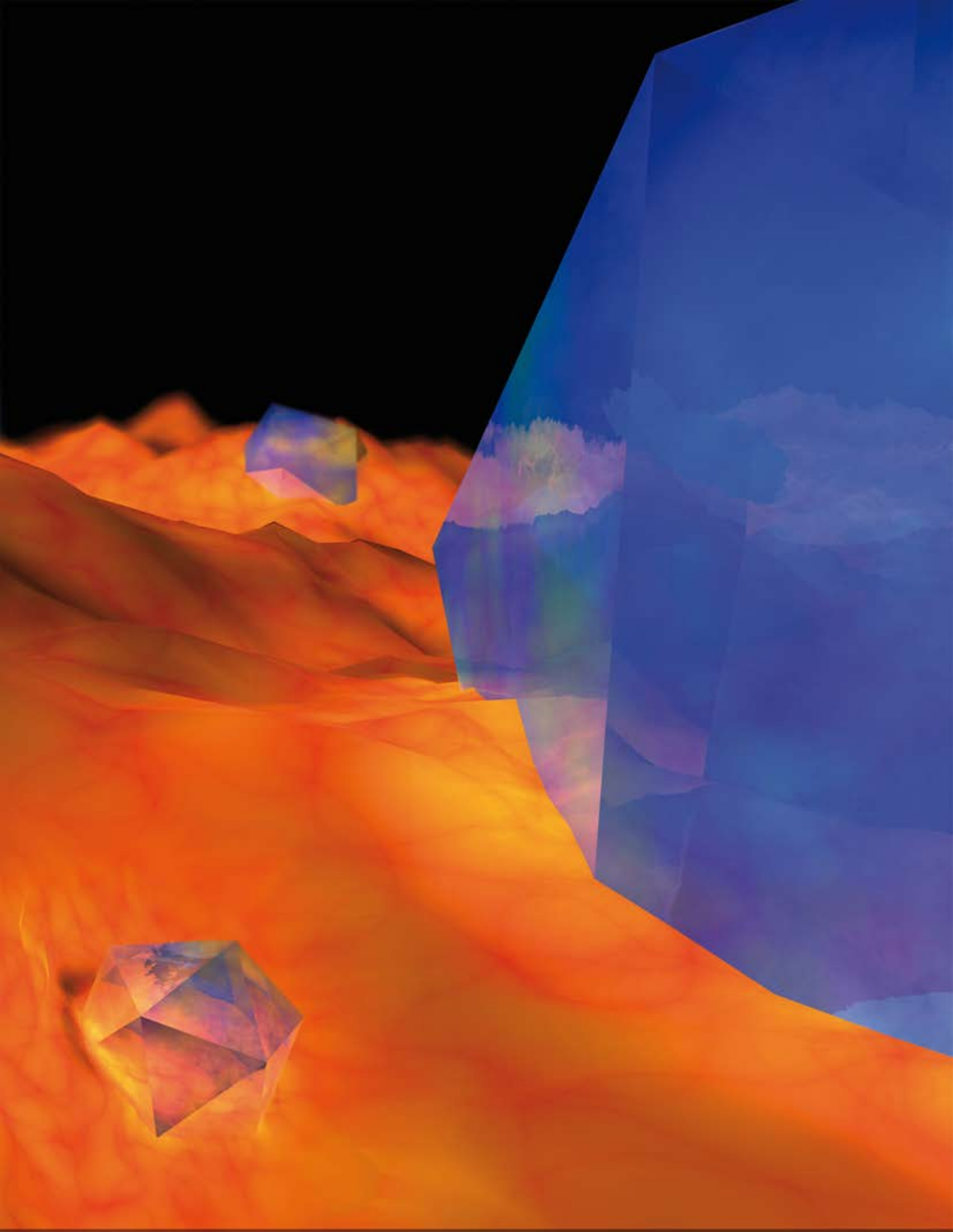

Artwork Quasicrystals in fiery matrix, F. Formica, Cartilage Engineering & Regeneration, D-HEST
Layout M.A. Heinrich, Optical Materials Engineering Lab, D-MAVT